6 *Growth analysis: a quantitative approach*

...and he gave it for his opinion, that whosoever would make two ears of corn or two blades of grass to grow where only one grew before would deserve better of mankind, and do more essential service to his country, than the whole race of politicians put together...

(Jonathan Swift, Gulliver's Travels, 1726)

Highly productive multiple cropping in a CO_2-enriched greenhouse at CSIRO Merbein, 1978
(Original photograph courtesy Ted Lawton)

Chapter outline

Introduction

Growth analysis is a conceptual framework for resolving the nature of genotype × environment interactions on plant growth and development. In natural environments, growth and development cycles have to be completed within a time frame dictated by environmental conditions where light, moisture and nutrients often limit expression of genetic potential. Adaptive features that counter such constraints and help sustain relative growth rate can be revealed via growth analysis under contrasting conditions.

In managed environments, crop plants commonly experience similar restrictions, but in addition their economic yield is often only a small portion of total biomass at harvest and subject to internal (genetic) control. Whole-plant growth analysis is therefore of interest to those concerned with determinants of yield from crop plants growing singly or as communities.

Accordingly, in their quest for improved genotypes crop scientists often need to explore plant growth and reproductive development in quantitative terms. Sources of variation in productivity can then be resolved into those processes responsible for converting external resources into biomass and those responsible for partitioning biomass into usable sinks such as cereal ears or pumpkins. Both aspects are addressed here.

6.1 Concepts and techniques

Growth models developed from populations of single cells can be extended mathematically to cover complex multicellular organisms where whole-plant growth is expressed in terms of leaf area and nutrient resources. Such growth indices are not intrinsic properties of plants, but rather mathematical constructs with functional significance. These concepts can be traced to the early 1900s and have proved increasingly useful for studies of growth and developmental responses in natural and managed environments.

6.1.1 Cell populations

A small population of unicellular organisms presented with abundant resources and ample space will increase exponentially (Figure 6.1a). Population doubling time T_d (hours or days) is a function of an inherent capacity for cell division and

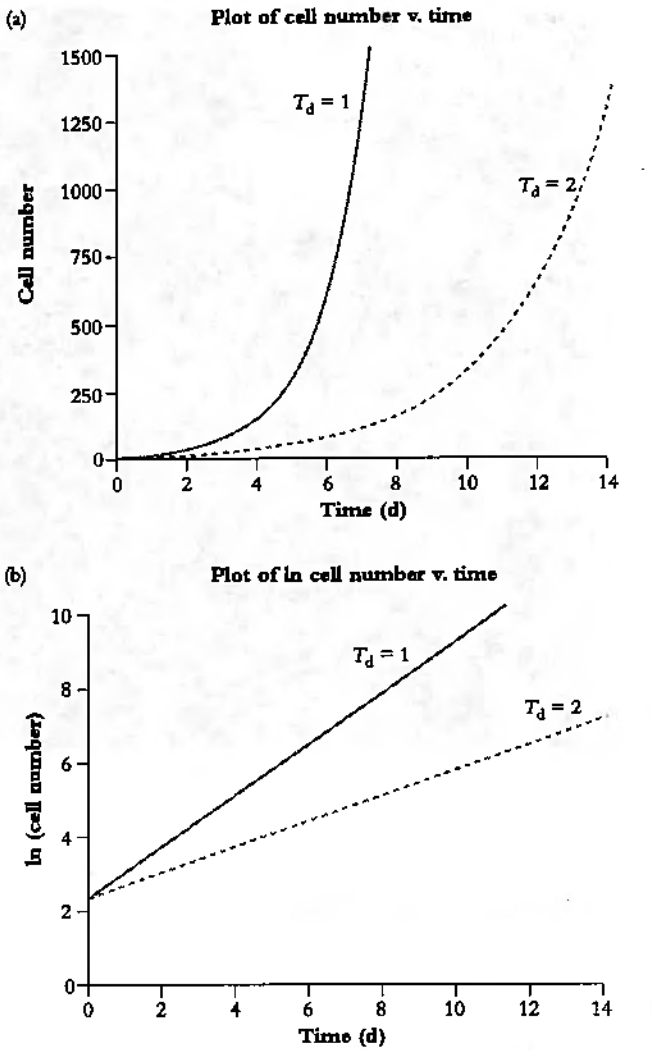

Figure 6.1 A population of cells unrestricted by space or substrate supply will grow exponentially. In this hypothetical case, a fast-growing strain of a single-celled organism with a doubling time of 1 d (relative growth rate (RGR) of 0.6932 d^{-1}) starts on day 0 with a population of n cells which increases to $128.n$ by day 7. The slow-growing strain with a doubling time of 2 d (RGR = 0.3466 d^{-1}) takes twice as long to reach that same size. When data for cell numbers are ln-transformed, exponential curves (a) become straight lines (b) where slope = RGR

enlargement which is expressed according to environmental conditions, and in Figure 6.1(a) doubling times for these two populations are 1 and 2 d for fast and slow strains respectively.

Exponential curves such as those in Figure 6.1(a) can be expressed as

$$N(t) = N_0\, e^{rt} \qquad (6.1)$$

where $N(t)$ is the number of cells present at time t, N_0 is the population at time 0, r determines the rate at which the

population grows, and e (or Euler's number) is a transcendental number where e = 2.7182 and is also the base of natural logarithms. By derivation from Equation 6.1

$$r = \frac{1}{N}\frac{dN(t)}{dt} \tag{6.2}$$

and accordingly is called **relative growth rate** with units of 1/time. Doubling time can be shown to be $T_d = (\ln 2)/r$.

If a population or an organism has a constant relative growth rate then doubling time is also constant, and that population must be growing at an exponential rate given by Equation 6.1. The 'fast' strain in Figure 6.1(a) is doubling every day whereas the 'slow' strain doubles every 2 d, thus r is 0.6932 d^{-1} and 0.3466 d^{-1}, respectively.

If cell growth data in Figure 6.1(a) are converted to natural logarithms (i.e. ln transformed), two straight lines with contrasting slopes will result (Figure 6.1b). This application of ln transformation is a crucial concept in growth analysis, providing a basis for calculation of growth indices discussed later. For strict exponential growth where $N(t)$ is given by Equation 6.1, it follows that

$$\ln N(t) = \ln N_0 + rt \tag{6.3}$$

so that a plot of ln $N(t)$ as a function of time t is a straight line whose slope is relative growth rate r.

In practice, r is inferred by assessing cell numbers N_1 and N_2 on two occasions t_1 and t_2 (separated by hours or days depending on doubling time — most commonly days in plant cell cultures), and substituting those values into the expression

$$r = \frac{\ln N_2 - \ln N_1}{t_2 - t_1} \tag{6.4}$$

which expresses r in terms of population numbers N_1 and N_2 at times t_1 and t_2, respectively.

If relative growth rate r is not constant, then growth is not exponential but the concept of relative growth rate is still useful for atualysis of growth dynamics in populations or organisms. Equation 6.3 is then used to compute average relative growth rate between times t_1 and t_2 even though population growth might not follow Equation 6.1 in strict terms. In that case plots analogous to Figure 6.1(b) will not be straight lines.

6.1.2 Plant biomass

Apart from some specialised applications in leaf expansion, organ enlargement or *in vitro* culture of cell suspensions, cell number is an impractical measure of growth in whole plants. Instead, fresh or oven-dried biomass (W) is generally taken as a surrogate for carbon gain and referenced to the number of days elapsed between successive observations. At any instant, relative growth rate, RGR (d^{-1}) can be expressed in terms of differential calculus as RGR = $(1/W)(dW/dt)$ (compare Equation 6.2.) so that RGR is increment in dry mass (dW) per increment in time (dt) divided by existing biomass (W). Averaged over a time interval t_1 to t_2 during which time biomass increases from W_1 to W_2, RGR (d^{-1}) can be calculated from

$$\text{RGR} = \frac{\ln W_2 - \ln W_1}{t_2 - t_1} \tag{6.5}$$

RGR at any instant can also be expressed in terms of differential calculus as RGR = $(1/W)\ dW/dt$. This equation states that RGR is increment in dry mass (dW) per increment in time (dt) divided by existing biomass (W).

Net gain in biomass (W) is clearly an outcome of CO_2 assimilation by leaves minus respiratory loss by the entire plant. Leaf area can therefore be viewed as a driving variable, and biomass increment (dW) per unit time (dt) can then be divided by leaf area (A) to yield the net assimilation rate, NAR (g m^{-2} d^{-1}), where

$$\text{NAR} = \frac{1}{A}\frac{dW}{dt} \tag{6.6}$$

Averaged over a short time interval (t^1 to t_2 days) and provided whole-plant biomass and leaf area are linearly related (see Radford 1967 and literature cited),

$$\text{NAR} = \left(\frac{W_2 - W_1}{t_2 - t_1}\right)\left(\frac{\ln A_2 - \ln A_1}{A_2 - A_1}\right) \tag{6.7}$$

NAR thus represents a plant's net photosynthetic effectiveness in capturing light, assimilating CO_2 and storing photoassimilate. Variation in NAR can derive from differences in canopy architecture and light interception, photosynthetic activity of leaves, respiration, transport of photoassimilate and storage capacity of sinks, or even the chemical nature of stored products.

Since leaf area is a driving variable for whole-plant growth, the proportion of plant biomass invested in leaf area or 'leafiness' will have an important bearing on RGR, and can be conveniently defined as leaf area ratio, LAR (m^2 g^{-1}), where

$$\text{LAR} = \frac{A}{W} \tag{6.8}$$

At any instant, or in practice at any harvest, LAR can be taken as A/W and can be factored into two components, namely specific leaf area (SLA) and leaf weight ratio (LWR). SLA is simply a 'ratio' of leaf area (A) to leaf mass (W_L) (dimensions m^2 g^{-1}) and LWR is a true ratio of leaf mass (W_L) to total plant mass (W) (dimensiouless). Thus,

$$\text{LAR} = \frac{A}{W_L}\frac{W_L}{W} \tag{6.9}$$

$$= \text{SLA} \times \text{LWR}$$

Alternatively, and as commonly employed for growth analysis, average LAR over the growth interval t_1 to t_2 is simply

$$\text{LAR} = \tfrac{1}{2}\left(\frac{A_1}{W_1} + \frac{A_2}{W_2}\right) \quad (6.10)$$

Expressed this way, LAR becomes a more meaningful growth index than A/W (Equation 6.8) and can help resolve sources of variation in RGR. If both A and W are increasing exponentially so that W is proportionl to A, it follows that

$$\frac{1}{W}\frac{dW}{dt} = \frac{1}{A}\frac{dW}{dt} \times \frac{A}{W} \quad (6.11)$$

or summarised in terms of now familiar growth indices,

$$\text{RGR} = \text{NAR} \times \text{LAR} \quad (6.12)$$

or more explicitly,

$$\text{RGR} = \text{NAR} \times \text{LWR} \times \text{SLA}. \quad (6.13)$$

In practice, such ideal conditions are only rarely met, and these multiplier-product relationships must be applied with caution (see especially Williams 1946 and Radford 1967). Nevertheless, where valid application is possible, sources of variation in RGR can be partitioned between NAR, LWR and SLA, or simply between NAR and LAR. Such outcomes provide particularly useful insights on driving variables in process physiology and ecology.

Basic concepts of classic plant growth analysis as described above apply to individuals, and ideall, those growth indices would be derived from non-destructive assay. Experimentally, a population of fast-growing (small) plants is sampled at frequent intervals, and sample means are then taken as representative of the population. Relatively few harvests (commonly weekly) but relatively large numbers of replicates (commouly six to eight plants) are employed. Harvested plants are subdivided into component parts while still fresh, leaf area is measured, and all biomass subsequently oven dried for dry mass determination. An error estimate for RGR can be calculated by pairing plants across harvests, that is, taking the largest plant at t_1 and the largest at t_2 and calculating RGR, then the next-largest pair and so on. Mean RGR and variance are then derived (see Poorter (1989) for more discussion on pairing, and Poorter and Lewis (1996) for more on sampling methods).

Functional growth analysis

Classic plant growth analysis continues to find application in resolving sources of variation in RGR but suffers from statistical deficiencies and strict prerequisities for valid application of the formnlae discussed above. Functional growth analysis was developed during the 1960s to overcome these limitations and was made feasible with the advent of computer-based data analysis at about that time. In this technique (see Hunt 1982) curves generated by mathematical functions are fitted to both A and W (either original values or ln-transformed data). RGR at any particular point in time is then calculated as the slope of ln W versus time. Other indices can be calculated once an adequate relationship between ln A and time is established. In effect, an adequate relationship between ln W and ln A versus time allows calculation of instantaneous values for RGR, NAR and LAR. As mentioned above, the slope of ln W versus time yields RGR, and at that same instant A can be derived from the ln A versus time relationship, allowing LAR (A/W) to be calculated. With RGR already derived, NAR is then RGR/LAR.

Functional growth analysis enables experimenters to follow a time-course in growth indices and to derive instantaneous values. In practical terms, large harvests at weekly intervals are no longer needed. Instead, smaller harvests of two to four plants every 3–4 d are sufficient. However, data analysis remains critical, and especially important is choice of a mathematical function with biologically meaningful parameters that best fits ln-transformed values (see Hunt 1978, 1982 for further details).

Growth indices in summary

Whole-plant growth is amenable to analysis via either classic or functional methods. In either case, five key indices are commonly derived as an aid to understanding growth responses. Mathematical and functional definitions of those terms are summarised below.

Growth index	Mathematical definition	Units	Functional definition
Relative growth rate RGR	$1/W\ dW/dt$	d^{-1}	Rate of mass increase per unit mass present (efficiency of growth with respect to mass)
Net assimilation rate NAR	$1/A\ dW/dt$	$g\ m^{-2}\ d^{-1}$	Rate of mass increase per unit leaf area (efficiency of leaves in generating biomass)
Leaf area ratio LAR	A/W	$cm^2\ g^{-1}$	'Ratio' of leaf area to total plant mass (a measure of 'leafiness' or of photo synthetic surface relative to respiratory mass)

continued

Growth index	Mathematical definition	Units	Functional definition
Specific leaf area SLA	A/W_L	$cm^2\ g^{-1}$	'Ratio' of leaf area to leaf mass (a measure of relative thickness, density or spread of leaves)
Leaf weight ratio LWR	W_L/W		Ratio of leaf mass to total plant mass (a measure of biomass allocation to leaves)

LAR and SLA both carry dimensions of $cm^2\ g^{-1}$ (or $m^2\ kg^{-1}$) and are therefore not true ratios as implied by the term 'ratio'. LWR is a true dimensionless ratio. The reciprocal of SLA, or leaf mass per unit leaf area, is often but mistakenly referred to as specific leaf weight (SLW). By definition, any 'specific' index must be referenced to mass, so that SLW will always equal 1 (Jarvis 1985). For that reason, and where such data warrant inclusion, leaf mass to leaf area 'ratio' will be used rather than SLW.

6.1.3 Leaf area

(a) Patterns of cell division and cell enlargement

LAR can be an important driving variable for whole-plant growth so that dynamics of leaf expansion will underpin RGR responses to genetic and environmental effects. Indeed, variation in LAR is frequently perceived as impacting more directly on whole-plant growth than variation in NAR. Accordingly, leaf growth deserves some attention in this present context of plant growth analysis.

Leaves are first discernible as tiny primordia which are initiated by meristems in strict accord with a genetically programmed developmental morphology. As shoot growth proceeds, dicotyledonous primordia undergo extensive cycles of cell division (peak doubling time *c.* 0.5 d) emerging as recognisable leaves that unfold and expand. Lamina expansion follows a coordinated pattern of cell division and cell enlargement that is under genetic control but modified by the environment. Final leaf size and shape vary accordingly.

Leaf growth in grasses (monocotyledons) such as rice, wheat, coarse grains and pasture grasses is qualitatively different from that in broad-leafed plants (dicotyledons) such as sunflower, cucurbit, tobacco and pasture legumes. Primordia of dicotyledons bear a superficial resemblance to those of monocotyledons, but as grass leaves emerge cell division is confined to basal meristems which give rise to a zone of cell expansion. Leaf maturation proceeds from tip to base. Cell division and cell enlargement proceed concurrently, but are separated spatially. By contrast, broad-leafed plants show more of a temporal separation where a phase of cell division precedes a subsequent phase of cell enlargement (but with some overlap as discussed later). Notwithstanding such distinctions in cell growth dynamics, the net outcome for area increase is similar. Lamina expansion in both monocotyledons and dicotyledons is approximately sigmoidal in time and asymmetric about a point of inflexion which coincides with maximum rate of area increase.

Taking cucumber as an archetype for dicotyledonus leaves (Figure 6.2), this inflexion point occurs later under lower irradiance (compare data on leaf area increase under 0.6 with 4.4 MJ $m^{-2}\ d^{-1}$ in Figure 6.2). Early expansion of leaf primordia is driven primarily by cell division, and cell number per leaf increases exponentially prior to unfolding (solid lines in Figure 6.2). Rate of cell division during this early phase is increased by irradiance, so that potential size of these cucumber leaves at maturity is also enhanced. Using the upper curves in Figure 6.2 as an example (highest irradiance), cell number per

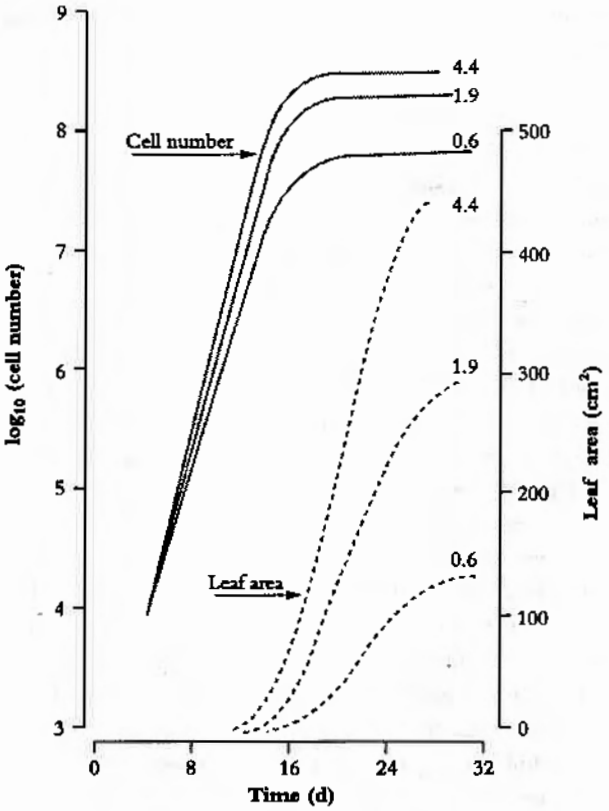

Figure 6.2 Leaves of cucumber (node 2 on plants in growth cabinets) show an approximately sigmoidal increase in area with time (broken lines) where final size and cell number vary with daily irradiance (0.6, 1.9 or 4.4 MJ $m^{-2}\ d^{-1}$). During an initial exponential phase in area growth, cell number per leaf (solid lines) also increases exponentially. The slope of a semi-log plot (hence relative rate of cell division) is higher under stronger irradiance. Cell number per leaf approaches an asymptote (cell division slows) as leaf area increase becomes linear
(Based on Milthorpe and Newton 1963)

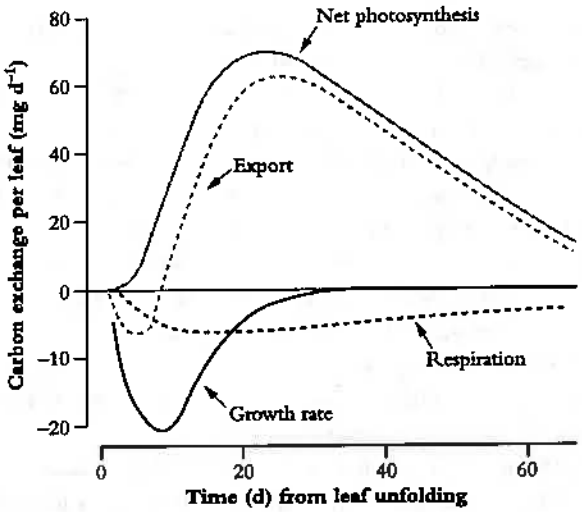

Figure 6.3 Carbon exchange by a cotton leaf (node 7 main stem under cloudy conditions; photon irradiance 17 mol quanta m^{-2} d^{-1}) shows a peak in both net photosynthesis and export of photoassimilate as leaf growth (expansion) slows. An initial phase of carbon import helps sustain early expansion (shown here as a negative export). Positive export of photoassimilate is evident after about 9 d, coinciding with rapid expansion and a time of maximum carbon investment in leaf growth. (Note expanded scale for growth and respiration)
(Based on Constable and Rawson 1980)

lamina reaches a plateau around 20 d, but area continues to increase to at least 30 d. Clearly, cell expansion is largely responsible for lamina expansion between 20 and 30 d after sowing.

While the initial (exponential) phase of dicotyledonous leaf growth is driven largely by cell division, and the subsequent (asymptotic) phase is largely due to enlargement of the resulting cell population, the distinction between these two phases is somewhat arbitrary. Improved techniques for tissue maceration and cell counting have shown that cell division can continue well into the cell-expansion phase of leaf growth. Formation of such new cells is conservative, but does mean that about 90% of cells in a mature cucumber leaf can originate subsequent to unfolding. Data for tobacco and sunflower are closely comparable to those shown here for cucumber (see Table 2 in Dale 1982).

Contrasting time-courses for cell division and subsequent eulargement hold implications for leaf function. For example, epidermal layers usually cease division ahead of mesophyll tissues so that leaf thickness can increase for some time after leaves reach full size (Dale 1976, 1982) and by implication have a greater depth of photosynthetic tissue. Typically, photosynthetic capacity will reach a maximum just before leaves reach full size (Figure 6.3) although export of photosynthetic products does not peak until leaves are at full size (dashed line in Figure 6.3). Cell division has normally ceased at that stage (see Table 6 in Dale 1976).

(b) Resources for cell division and cell enlargement

In leaves of both dicotyledons and monocotyledons, cell number dictates potential size, but expression of that potential is determined by cell enlargement, and these two phases of lamina expansion have distinct needs. Cell division is substrate intensive but cell enlargement is not, and carbon requirement for later phases of leaf growth is demonstrably small. In cotton, for example (Figure 6.3) local photosynthesis plus some imported substrate were necessary for early expansion but a net export of photoassimilate was apparent within only 7–8 d of unfolding. Respiratory losses were at most only 10% of daily fixation with remaining photoassimilate going to export.

During leaf expansion, volumes of constituent cells can increase 10–100-fold depending upon location and function, cells such as spongy mesophyll showing the greatest increase and guard cells the least. Photoassimilate is readily available and generally sufficient (discussed above) but a positive turgor must be sustained for cell enlargement and leaf expansion which in turn depends on water plus inorganic resources that must all be imported. A reliable supply of nitrogen, phosphorus, potassium and magnesium is crucial (Dale 1982) and especially significant for synthetic events within enlarging cells. Chloroplast replication in spinach is a case in point where plastid numbers per cell increase from 10 or 20 at leaf unfolding up to 200 per cell in full-sized leaves (Possingham 1980).

Nutrient requirements to sustain such prodigious syntheses are substantial, and again taking cucumber as indicative of broad-leafed plants Milthorpe (1959) demonstrated that rate of leaf production (and by impliction cell division in terminal meristems) was comparatively insensitive to depletion of external nutrients whereas expanding leaves had a high demand. Similarly leaf growth in subterranean clover (*Trifolium subterraneum*) proved more sensitive to potassium and magnesium deficiency than did photosynthesis, so that photoassimilate actually accumulated in nutrient-deficient plants (Bouma *et al.* 1979).

(c) Mathematical analysis of leaf expansion

The collective activities of cells in an expanding lamina are amenable to mathematical analysis. Despite differences between monocotyledons and dicotyledons in spatial and temporal patterns of leaf growth, as well as differences between dividing cells and enlarging cells in their requirements for carbon and nutrients, growth curves for single leaves can prove instructive.

Differences in canopy development (genetic or environmental causes) can be attributed to three sources, namely. (1) frequency of new leaf initiation, (2) size of primordia and (3) time-course of lamina expansion. All three sources can be inferred to some extent from comprehensive measurement of lamina expansion by successive leaves, and a determinate plant such as sunflower (Figure 6.4) provides a convenient example. The curves in Figure 6.4 were drawn by hand through all data points (two measurements of leaf length (L) and leaf breadth (B) per week with area (A) estimated from the relationship $A = 0.73\ (L \times B)$. Leaf area (A) is shown as a function of time for eight nodes selected between node 6 and node 40.

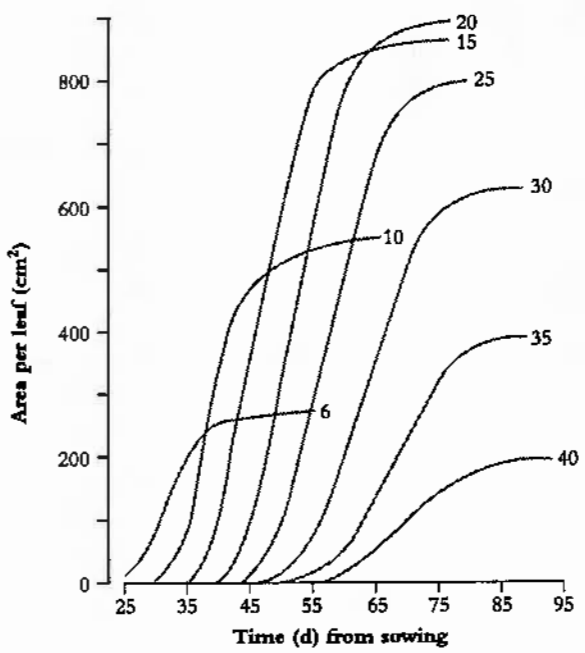

Figure 6.4 Leaf expansion in sunflower shows a sigmoidal increase in lamina area with time where relative rate of area increase (r) and final size (A_m) both vary with nodal position, reaching a maximum around node 20
(Based on Rawson and Turner 1982)

Curves change shape in a characteristic fashion according to node position, and carry important implications for underlying growth processes. Node 20 produced the largest leaf on this plant, while slowest growth and smallest final size was recorded for node 40 (adjacent to the terminal inflorescence).

Frequency of leaf initiation can be inferred from a more comprehensive family of such curves where early exponential growth in area for each successive leaf is recorded and plotted as $\log_{10}$ area versus time. This results in a near-parallel set of lines which intersect an arbitrary abscissa (Figure 6.5). Each time interval between successive points of intersection on this abscissa is a 'phyllochron' and denotes the time interval between comparable stages in the development of successive leaves. This index is easily inferred from the time elapsed between successive lines on a semi-log plot (Figure 6.5).

Figure 6.5 Leaves of subterranean clover achieve a 10-million-fold increase in size from primordium to final area (volume of primordia shown as dotted lines; leaf fresh mass shown as solid lines). Successive leaves are initiated and enlarge in a beautifully coordinated fashion revealed here as a family of straight lines on a semi-log plot. Intervals along an arbitrary abscissa (arrow at 100×10^{-3} mm³) that intersects these lines represent time elapsed (about 1.8 d) between attainment of a given developmental status by successive leaves (phyllochron)
(Based on Williams 1975)

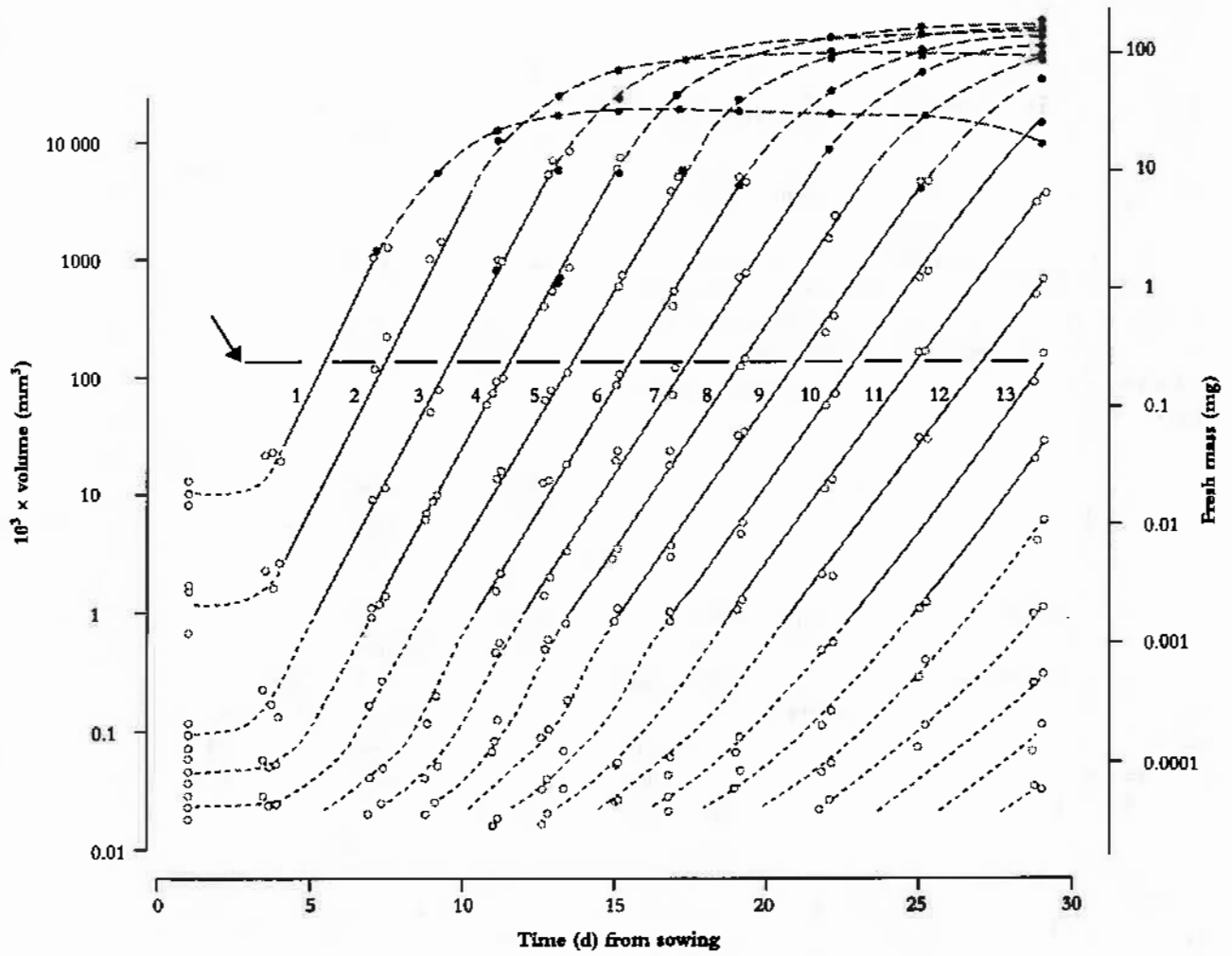

Cumulative phyllochrons serve as an indicator of a plant's physiological age in the same way as days after germination represent chronological age.

The dynamics of lamina expansion following leaf unfolding in dicotyledons, or of leaf extension in monocotyledons, is a third and most definable source of variation in canopy development. Each leaf follows a qualitatively similar time-course (e.g. Figure 6.5) and is commonly described by a Richards (1959, 1969) function reparameterised by Cromer *et al.* (1993) to yield:

$$A(t) = A_X(1 + d\, e^{r(t-t_0)(1+d)})^{-1/d} \qquad (6.14)$$

The four parameters A_X, t_0, r and d have a clear geometric meaning. A_X (cm^2) stands for the final area attained by a leaf, and is the asymptotic value for A at large t, t_0 (d) is the time when $A(t)$ undergoes inflexion from initially exponential to subsequently asymptotic increase, r (d^{-1}) is relative rate of area increase by a leaf (RGR_{AREA}) with an area of $A(t)$ at t_0, and d determines the shape of the curve of A versus t (larger d results in an inflexion point higher up the curve).

Mathematical analysis of leaf expansion now becomes a vehicle for defining environmental effects on canopy development, or for making genetic comparisons. Some examples of environmental effects on $A(t)$ and r are given later (Section 6.2).

6.2 Environmental physiology

Light, CO_2, temperature, water and nutrients are taken as key driving variables for growth responses in a wide range of species. Growth indices, especially whole-plant and leaf RGR, serve as an indicator of plant response and of interactions between environmental factors where they occur. Variation in whole-plant RGR is then resolved into contributions from NAR and LAR. Ecological implications for managed and natural communities are considered.

6.2.1 Light

Light impacts on both extent and activity of plant canopies. Taking cucumber as an archetype for herbaceous crop plants (Figure 6.6) leaf growth increases with daily irradiance due to increased cell number rather than increased cell size. Leaf thickness is also positively affected by daily irradiance, principally resulting in a greater depth of palisade (Table 6.1). Indeed, mean cell volume is more than doubled under strong irradiance (3.11×10^{-5} mm^3 at 3.2 MJ m^{-2} s^{-1} cf. 1.46×10^{-5} mm^3 at 0.5 MJ m^{-2} d^{-1} in Table 6.1), and because cross-sectional area is virtually unchanged cell depth is responsible. This greater depth of palisade in strong light confers a greater photosynthetic capacity on such leaves (expressed on an area basis) and translates into larger values for NAR and a potentially higher RGR. At lower irradiance (Table 6.1) leaves are thinner and SLA will thus increase with shading, and because LAR = SLA × LWR (recall Equation 6.9) a smaller absolute size at lower irradiance can be offset by larger SLA resulting in LAR increase.

Table 6.1 Leaf size and other physical attributes measured on Cucumis sativus *foliage at node 3 show a positive response to daily irradiance in growth cabinets*

Attribute	Daily irradiance (MJ m^{-2})	
	0.5	3.2
Area of leaf (cm^2)	127	356
Leaf thickness (μm)		
Sections	88	211
Vol./area	111	222
Mean cell volume (10^4 μm^3)	1.46	3.11
Cell cross-section (μm^2)	131	138

(Adapted from Wilson 1966)

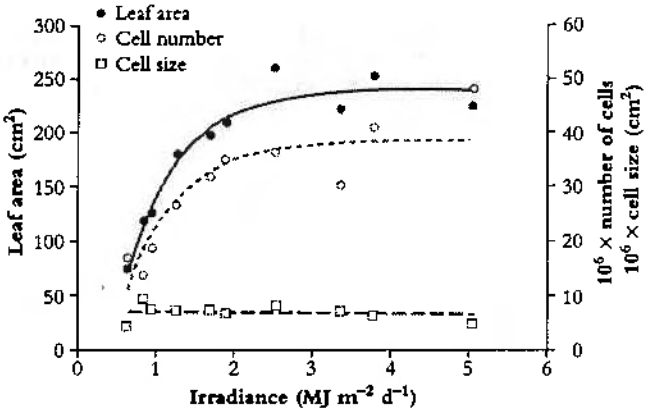

Figure 6.6 Area of individual leaves on cucumber (*Cucumis sativus*) responds to daily irradiance and reaches a maximum above about 2.5 MJ m^{-2} d^{-1}. Area increase (node 2 in this example) is due to greater cell number under stronger irradiance. Mean size of mesophyll cells is little affected and has no influence on area of individual leaves.
(Based on Newton 1963)

G. E. Blackman (Agriculture Dept Oxford University) appreciated the significance of such LAR × NAR interaction for whole-plant growth, and in a series of comprehensive papers with a number of collaborators documented shade-driven growth responses for many species. RGR response to growing conditions such as shade, and the degree to which upward adjustment in LAR could offset reduced NAR, was a recurring theme. Plants were commonly held in either full sun or under combinations of spectrally neutral screens that reduced daily irradiance to either 24% or 12% of full sun. These three treatments commenced with onset of rapid growth by established seedlings, and harvests taken as plants were judged to have doubled in size over successive intervals. Steady exponential growth ensured that treatment effects on RGR could be resolved into component responses by NAR and LAR.

In a series of 20 pot experiments, Blackman and Wilson (1951a) first established a close relationship between NAR

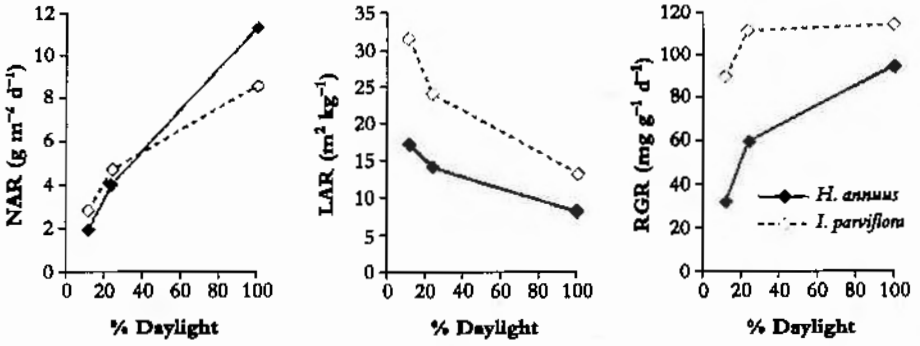

Figure 6.7 A sun-adapted plant such as *Helianthus annuus* adjusts LAR to some extent in response to lower daily irradiance but not enough to maintain RGR. By contrast, a shade-adapted plant such as *Impatiens parviflora* with somewhat higher LAR and RGR in full sun makes further adjustment in LAR so that RGR does not diminish to the same extent in moderate or deep shade as does that of *H. annuus*
(Based on Blackman and Wilson 1951b; Evans and Hughes 1961)

and daily irradiance where shade-dependent reduction in NAR was similar for 10 species. More precisely, NAR was linearly related to log irradiance and extrapolation to zero NAR corresponded to a light-compensation point of 6–9% full sun for eight species, and 14–18% full sun for two others. Significantly, neither slope nor intercept of NAR versus. $\log_{10}$ daily irradiance differentiated sun-adapted plants such as barley, tomato, peas and sunflower from two shade-adapted species (*Geum urbanum* and *Solanum dulcamara*). LAR proved especially responsive to light and accounted for contrasts between sun plants and shade plants in their growth response to daily irradiance.

Concentrating on sunflower seedlings, Blackman and Wilson (1951b) confirmed that NAR increased with daily irradiance (Figure 6.7a) and that LAR was greatly increased by shading especially in young seedlings (uppermost line in Figure 6.7b). Response in RGR tracked LAR and especially in young seedlings which also showed highest RGR and were most sensitive to shading. LAR appeared sensitive to both daily maxima as well as daily total irradiance. Variation between species in adjustment to shade, and ultimately their long-term shade tolerance, would then derive from plasticity in LAR.

A subsequent comparision between sunflower and the woodland shade plant *Impatiens parviflora* by Evans and Hughes (1961) confirmed this principle of LAR responsiveness to irradiance (Figure 6.7). Sunflower achieved noticeably higher NAR in full sun than did *I. parviflora*, but LAR was considerably lower and ironically translated into a somewhat slower RGR for sunflower. This species contrast was, however, much stronger in deep shade (12% full sun) where RGR for *I. parviflora* had fallen to 0.090 d^{-1} whereas sunflower was only 0.033 d^{-1}. Clearly, *I. parviflora* is more shade tolerant, and retention of a faster RGR in deep shade is due both to greater plasticity in LAR as well as a more sustained NAR. Adjustments in both photosynthesis and respiration of leaves contribute to maintenance of higher NAR in shade-adapted plants growing at low irradiance (Chapter 12).

A note on irradiance

Daily irradiance (photosynthetically active energy) at low to mid latitude (20–30°) can reach 15 MJ m^{-2} on clear days in midsummer. The tropics can be lower due to cloud cover, while at higher latitudes (30–50°) lower daily maxima are offset by long days. Plant growth and reproductive development vary accordingly, and some early results, including those from northern hemisphere experiments, must be viewed in this context. Warren Wilson (1966, 1967) analysed the performance of open-grown seedling sunflowers at Deniliquin and recorded the highest known value for NAR, namely 29.9 ± 0.4 g m^{-2} d^{-1}. Pooling data from Deniliquin and Oxford (Figure 6.8), NAR in widely spaced and nutrient-rich sunflower plants was linearly related to daily irradiance with a mean maximum NAR of about 25 g m^{-2} d^{-1} at about 15 MJ m^{-2} d^{-1}. In assimilatory terms, sunflower shows remarkable capacity and plasticity.

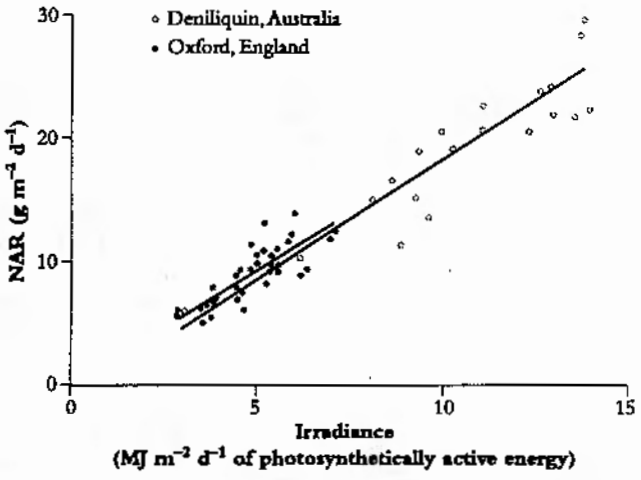

Figure 6.8 NAR for open-grown seedlings of sunflower (*Helianthus annuus*) responds linearly to daily irradiance across a wide range from low values recorded at Oxford to the highest recorded value for NAR of about 30 g m^{-2} d^{-1} at Deniliquin under a daily irradiance of 13.5 MJ m^{-2} d^{-1}
(Based on Warren Wilson 1969)

6.2.2 Temperature

Within a moderate temperature range readily tolerated by vascular plants (say *c.* 10–35°C) processes sustaining carbon gain show broad temperature optima. By contrast, developmental changes are rather more sensitive to temperature, and provided a plant's combined responses to environmental conditions do not exceed physiologically elastic limits (i.e. adjustments remain fully reversible) temperature effects on RGR are generally attributable to rate of canopy expansion rather than rate of carbon assimilation. In the early days of growth analysis, Blackman *et al.* (1955) inferred from a multi-factor analysis of growth response to environmental conditions that NAR was relatively insensitive to temperature, but whole-plant growth was obviously affected, so that extent (LAR) rather than performance per unit surface area (NAR) was responsible. Such inferences were subsequently validated.

Using day/night temperature as a driving variable, Potter and Jones (1977) provided a detailed analysis of response in key growth indices for a number of species (Table 6.2). Data for maize, cotton, soybean, cocklebur, Johnson grass and pigweed confirmed that 32/21°C was optimum for whole-plant relative growth rate (RGR_W) as well as relative rate of canopy area increase (RGR_A). Both indices were lowest at 21/10°C. Moreover, variation in RGR_W and RGR_A was closely correlated across species and treatments (pooled data).

All populations described in Potter and Jones (1977) maintained strict exponential growth. NAR could then be derived validly and temperature effects on NAR could then be compared with temperature effects on RGR_W and RGR_A (Figure 6.9). With day/night temperature as a driving variable, most values for NAR fell between 10 and 20 $gm^{-2}\ d^{-1}$. Correlation between NAR and RGR_W was poor (Figure 6.9a). By contrast, variation in both RGR_W and RGR_A was of a similar order and these two indices were closely correlated (Figure 6.9b).

Table 6.2 Relative rate of whole-plant growth ($RGR_W\ d^{-1}$) and relative rate of canopy expansion ($RGR_A\ d^{-1}$) (obtained via functional growth analysis) are both sensitive to day/night temperature regime with a broad optimum around 32/21°C. RGR_W and RGR_A were higher in C_4 than in C_3 species, and especially under warm conditions

Species	Pha mode	21/ RGR_W	10°C RGR_A	32/ RGR_W	21°C RGR_A	38/ RGR_W	27°C RGR_A
Cotton	C_3	0.086	0.073	0.206	0.197	0.188	0.172
Soybean	C_3	0.108	0.124	0.202	0.199	0.165	0.168
Cocklebur	C_3	0.165	0.151	0.269	0.263	0.204	0.176
Maize	C_4	0.096	0.133	0.255	0.354	0.178	0.189
Johnson grass	C_4	0.156	0.139	0.391	0.370	0.359	0.324
Pigweed	C_4	0.262	0.239	0.482	0.436	0.393	0.328

(Adapted from Potter and Jones 1977)
Cotton, *Gossypium hirsutum* L.; soybean, *Glycine max* [L.] Merr.; cocklebur, *Xanthium pensylvanicum* Wallr.; maize, *Zea mays* L.; Johnson grass, *Sorghum halepense* [L.] Pers.; pigweed, *Amaranthus retroflexus* L.

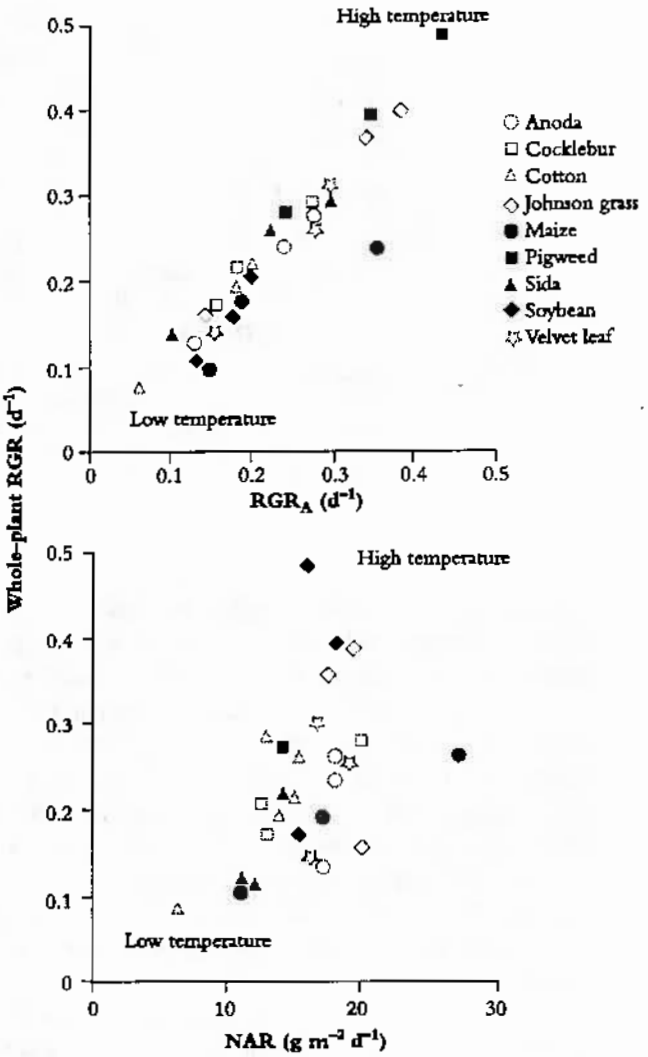

Figure 6.9 Variation in whole-plant RGR is linked to relative rate of canopy expansion (RGR_A). Nine species (including C_3 and C_4 plants) grown under three temperature regimen (21/10°C, 32/21°C and 31/27°C day/night) expressed wide variation in RGR that showed a strong correlation with RGR_A, but was poorly correlated with variation in NAR. Extent rather than activity of leaves appears to be more important for RGR response to temperature
(Based on Potter and Jones 1977)

Focusing on canopy expansion as a factor in RGR_W response to temperature, RGR_A is a composite index and refers to relative rate of canopy area increase by an entire plant. As explained earlier (Section 6.1.3) sources of variation in RGR_A include frequency of leaf initiation and appearance, rate of lamina expansion and final size of individual leaves. Temperature effects on whole-plant RGR_A can thus be resolved into component processes which correspond to parameters in Equation 6.14, namely Ax, r, t_0 and frequency of leaf appearance (phyllochron, derived by subtraction of t_0 for leaves on successive nodes). An example of temperature effects on those component processes is outlined in Table 6.3.

Wheat seedlings were raised at air temperatures of 6, 10 and 18°C and growth in area by successive leaves studied in detail. Recognising that leaf-growth dynamics and final size

vary with node (Figure 6.4) comparisons between these treatments are restricted to equivalent nodes. A_x from node 4 at 6°C is not recorded because plants grew so slowly that leaf 4 had still not emerged by the time this growth experiment was terminated. Leaves at node 2 did, however, attain full size but differed little between temperature treatments, while leaves from node 4 at 10°C and 18°C were also comparable. Unlike the positive effects of daily irradiance on final leaf size (Section 6.2.1), temperature effects on A_x were lacking in these wheat experiments. By contrast, relative rate of area increase (r) was strongly affected by temperature; and because A_x remained unchanged, duration of leaf growth must have been shortened. Similarly, appearance of new leaves was also accelerated under warm conditions; phyllochron decreased from 11 d at 6°C to only 3.5 d at 18°C.

Generalising from data in Table 6.3, positive effects of temperature on r and Δt_0 with little contribution from A_x will account for temperature effects on relative rate of canopy expansion by whole plants (RGR_A).

Table 6.3 Temperature enhances canopy growth in wheat via faster expansion of individual leaves (r) and faster appearance of successive leaves (shorter phyllochron Δt_0). Final size of individual leaves (A_x) is little affected

Temp. (°C)	Node	Final size A_x (cm^2)	RGR leaf r (d^{-1})	Phyllochron Δt_0 (d)
Expt 1				
6	2	205	0.095	11
	4	—	—	—
10	2	200	0.160	7.1
	4	320	—	—
18	2	193	0.290	3.5
	4	313	—	—
Expt 2				
6	3	250	0.096	13.0
10	3	250	0.171	6.50
14	3	252	0.253	4.33
18	3	247	0.316	3.25

(Adapted from Trought and Drew 1982; Trought, unpublished data)
In Expt 2, RGR leaf (r) represents a mean value for all leaves, and phyllochron is a mean value for intervals separating leaves at nodes 2–3 and nodes 3–4.

6.2.3 Carbon dioxide

Growth responses to elevated CO_2 can be spectacular, especially during early exponential growth (Figure 6.10a,b) and derive largely from direct effects of increased CO_2 partial pressure on photosynthesis. C_3 plants will be most affected, and especially at high temperature where photorespiratory loss of carbon has the greatest impact on biomass accumulation.

Global atmospheric CO_2 partial pressure is expected to reach 60–70 Pa (*c.* 600–700 ppm) by about 2050 so that growth response to a CO_2 doubling compared with 1990s levels has received wide attention (e.g. Cure and Acock 1986;

Figure 6.10 Early growth of cucumber (*Cucumis sativus*) (a) and wong bok (*Brassica pekinensis*) (b) is greatly enhanced in elevated CO_2 (1250 ppm) compared with ambient controls (325 ppm). As shown here, that initial effect is still apparent after 52 d of greenhouse culture in nutrient-rich potting mix. (Scale bar = 10 cm). (Further details in Kriedemann and Wong (1984) and adjacent table)
(Original photograph courtesy Maureen Whittaker)

Poorter 1993). Instantaneous rates of CO_2 assimilation by C_3 leaves usually increase two to three-fold but short-term response is rarely translated into biomass gain by whole plants where growth and reproductive development can be limited by low nutrients, low light, low temperature, physical restriction on root growth (especially pot experiments) or strength of sinks for photoassimilate. Given such constraints, photosynthetic acclimation commonly ensues (Chapter 13). Rates of CO_2 assimilation (leaf area basis) by CO_2-enriched plants, grown and measured under high CO_2, will match rates measured on control plants at normal ambient levels.

Acclimation takes only days to set in, and because plant growth analysis commonly extends over a few weeks, CO_2-driven responses in growth indices tend to be more conservative compared with instantaneous responses during leaf gas exchange. Moreover, C_4 plants will be less affected than C_3 plants (for reasons discussed in Chapters 2 and 13) so that broad surveys need to distinguish between photosynthetic mode. For example, in Figure 6.11, average NAR for 63 different cases of C_3 plants increased by 25–30% under 600–800 ppm CO_2 compared with corresponding values under 300–400 ppm CO_2. However, NAR increase was not matched by a commensurate response in RGR, and decreased

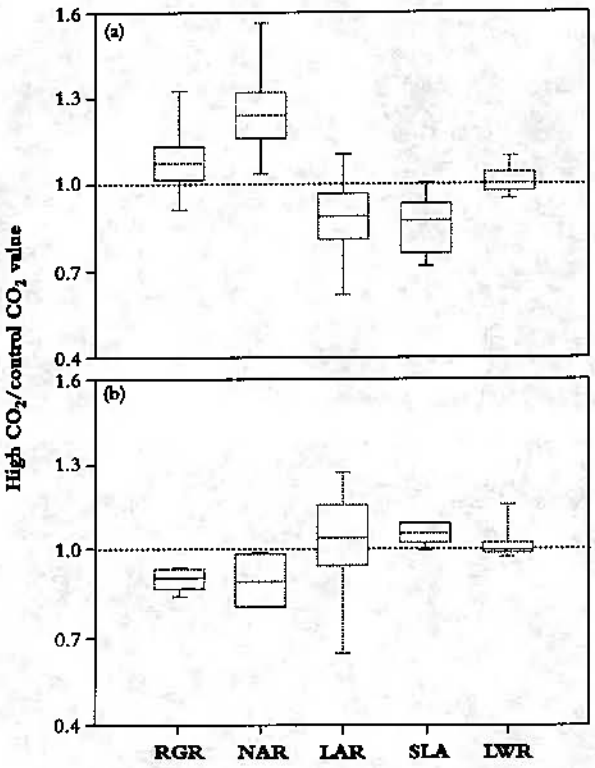

Figure 6.11 A survey of growth response to elevated CO_2 (ratio of growth indices in 600—800 cf. 300—400 ppm CO_2) in 63 different C_3 species (a) and eight C_4 species (b) reveals systematic differences in median values for growth indices that relate to photosynthetic mode. C_3 plants show a positive response in NAR that results in slightly faster RGR despite some reduction in LAR. C_4 plants reduce RGR under elevated CO_2 due to diminished NAR. SLA of C_3 plants is generally lower under elevated CO_2, but increased somewhat in C_4. LWR is essentially unchanged in either group
(Based on Poorter *et al.* 1996)

LAR appears responsible. CO_2-enriched plants were less leafy than controls (i.e. lower LAR), but not because less dry matter was allocated to foliage (LWR was on average unaltered). Rather, specific leaf area (SLA in Figure 6.11) decreased under high CO_2 so that a given mass of foliage was presenting a smaller assimilatory surface for light interception and gas exchange. Accumulation of non-structural carbohydrate (mainly starch; Wong 1990) is commonly responsible for lower SLA in these cases, and in addition generally correlates with down-regulation of leaf photosynthesis.

By contrast, in C_4 plants LWR was little affected by elevated CO_2, but in this case SLA did show slight increase with some positive response in LAR. However, photosynthetic acclimation may have been more telling because NAR eased and RGR even diminished somewhat under elevated CO_2.

Global change, with attendant increase in atmospheric CO_2 over coming decades, thus carries implications for growth and development in present-day genotypes and especially the comparative abundance of C_3 cf. C_4 plants (Chapter 13), but elevated CO_2 also has immediate relevance to greenhouse cropping. In production horticulture, both absolute yield and duration of cropping cycles are factors in profitability. Accordingly, CO_2 effects on rate of growth as well as onset of

Table 6.4 Brassica pekinensis (Wong Bok) and Cucumis sativus (Cucumber) are strongly affected by elevated CO_2 (ambient x 3.85) during early growth, but the response in both NAR and RGR becomes muted as plants grow. Canopy expansion (RGR_A) is especially sensitive to CO_2 enrichment, but only during early growth

Species	Age (d)	Ambient CO_2 RGR	NAR	RGR_A	Enriched CO_2 RGR	NAR	RGR_A
B. pekinensis	0–18	0.195	7.00	0.23	0.258	30.1	0.96
	18–24	0.307	9.77	0.297	0.291	11.8	0.222
	24–40	0.155	6.64	0.130	0.147	9.30	0.120
	40–52	0.114	8.1	0.061	0.066	6.65	0.020
C. sativus	0–21	0.107	6.93	0.164	0.173	13.3	0.215
	21–40	0.138	8.69	0.093	0.147	12.9	0.122
	40–52	0.036	3.27	0.061	0.051	5.80	0.035

(Adapted from Kriedemann and Wong 1984)
RGR (whole plant relative growth rate; d^{-1}
NAR (net assimilation rate; g m^{-2} d^{-1}
RGR_A (relative rate of canopy expansion; d^{-1}

reproductive development and subsequent development are of interest.

Young seedlings in their early exponential growth phase are typically most responsive to elevated CO_2, so that production of leafy vegetables can be greatly enhanced. This response is widely exploited in northern hemisphere greenhouse culture (e.g. Wittwer and Robb 1964) and was put to good effect in 'Head Start' programs at Beltsville (Krizek *et al.* 1974). In commercial operations, ambient CO_2 is often raised three- to four-fold so that growth responses can be spectacular (Figure 6.10a,b) but tend to be short lived (Table 6.4) as accelerated early growth gives way to lower RGR. During each cycle of growth and development, annual plants show a sigmoidal increase in biomass where an initial exponential phase gives way to a linear phase, eventually approaching an asymptote as reproductive structures mature. If CO_2 enrichment hastens this progression, a stage is soon reached where RGR is lower under elevated CO_2 due to accelerated ontogeny (see Gifford *et al.* 1996).

For example, wong bok (*Brassica pekinensis* in Figure 6.10b) is a highly productive autumn and winter vegetable that serves as 'spring greens' and is especially responsive to CO_2 during early growth. In present trials (Table 6.4) RGR_A at *c.* 330 ppm CO_2 was initially 0.230 d^{-1} compared with 0.960 d^{-1} at *c.* 1350 ppm CO_2, but by 40–52 d, RGR_A had fallen to 0.061 and 0.020 d^{-1} for control and CO_2 enriched, respectively.

CO_2-driven response in NAR and RGR also diminished with age, and especially where these larger individuals failed to sustain higher RGR past 18 d (Table 6.4). Nevertheless, a response in NAR was maintained for a further two intervals so that a CO_2 effect on plant size was maintained (Figure 6.10b).

Intensive greenhouse fruit crops such as tomato and cucumber are also raised under elevated CO_2, and as noted above for cucumber and leafy greens, young plants are especially responsive (and in tomato, even at low light; Hurd 1968; Hurd and Thornley 1974). Marketable yield of fruit is also

increased with CO_2-enriched plants commonly flowering earlier and producing about 30% more crop over a whole season with early cycles of reproductive development typically more responsive (50% increase; Madsen 1974). Photosynthetic acclimation in CO_2-enriched plants contributes to this diminished response over time, and has led to a management practice where CO_2-enriched greenhouses gradually revert to ambient as cropping seasons progress. An alternative strategy might be to 'pulse' greenhouses with CO_2 rather than enrich continuously, thereby forestalling photosynthetic acclimation. A duty cycle of 2 d enriched followed by 1 d ambient has been suggested (Kriedemann and Wong 1984).

Potato (*Solanum tuberosum* L.) offers an interesting variant in CO_2 effects on growth indices where differentiation of tubers provides sinks that can sustain NAR response to CO_2 (Table 6.5). In this experiment, over 400 potato plants were established in large containers of potting soil and held in a greenhouse (sunlight plus daylength extension to 15 h) under either ambient (300–370 ppm CO_2) or enriched conditions (600–700 ppm CO_2) from emergence to bloom (early enrichment 0–55 d; phase 1) or from bloom to final harvest (late enrichment 55–110 d; phase 2). Tuber yields at 55 d were increased significantly from 5.5 g plant^{-1} in control to 10.9 g plant^{-1} under CO_2 enrichment. Tuber number per plant was not significantly increased. By final harvest, tuber weight had increased to 17.5 and 22.0 g plant^{-1} for control and early enrichment respectively, but reached 30.5 g plant^{-1} in response to late enrichment (phase 2). Moreover, plants receiving late enrichment also sustained their NAR at 3.49 g m^{-2} d^{-1} during phase 2 compared with 1.77 in early-enriched plants and 1.91 in controls (Table 6.5). Presumably, photoassimilate generated by leaves during late enrichment with CO_2 was directed to tubers rather than accumulating in leaves and suppressing further assimilation. A stong ontogenetic progression was none the less evident in canopy development where relative rate of increase in leaf area per plant (RGR_A) dropped by an order of magnitude between phase 1 and phase 2, and also became insensitive to elevated CO_2.

Table 6.5 Tuber yield from Solanum tuberosum *(pot grown) is greatly enhanced by CO_2 enrichment subsequent to tuber differentiation. NAR responds to both early and late CO_2 enrichment, but relative rate of canopy expansion (RGR_A) is little affected at either stage*

	Phase 1 (0–55 d)	Phase 2 (56–110 d)
Tuber yield (g plant^{-1})		
Control	5.5	17.5
CO_2-enriched phase 1	10.9	22.0
CO_2-enriched phase 2	5.9	30.5
NAR (g m^{-2} d^{-1})		
Control	4.29	1.91
CO_2-enriched phase 1	5.74	1.77
CO_2-enriched phase 2	4.56	3.49
RGR_A (d^{-1} × 100)		
Control	5.79	0.77
CO_2-enriched phase 1	5.80	0.50
CO_2-enriched phase 2	5.60	0.53

(Adapted from Collins 1976)

6.2.4 Nutrients (nitrogen and phosphorus)

Leaf expansion is particularly sensitive to nutrient supply (especially nitrogen, phosphorus, potassium (N, P, K) and magnesium due primarily to the needs of enlarging cells for synthesis of new materials and generation of turgor. Reiterating assumptions made earlier (Section 6.1.3), an initial exponential phase in lamina expansion coincides with an especially active period of cell division, whereas the subsequent asymptotic phase is largely driven by cell enlargement. Relative rate of lamina expansion (r) at the end of that exponential phase is thus taken as indicative of cell division activity, whereas A_x reflects enlargement of that cell population. Nutrient deficiency or imbalance is first detected in leaf growth rather than leaf assimilation, and in terms of canopy development, nutrient supply impacts on phyllochron (Δt_0), relative rate of expansion (r) and final leaf size (A_x) (see Equation 6.14).

Such effects are nicely demonstrated by *Gmelina arborea* Roxb. (colloquially gmelina), a close relative of teak and favoured for tropical plantations by virtue of fast growth. Like teak, *G. arborea* carries large leaves that commonly grow to 750 cm^2 on high-quality sites. Leaves on greenhouse plants are smaller, but their growth dynamics are still informative. Plants grown on high, medium or low N supply (Table 6.6) with leaf [N] 2.94%, 1.18% and 0.63% N (dry mass) respectively show a strong decline in final size (A_x in Equation 6.14). By comparing high N with medium N, and noting little change in r (0.36 d^{-1} on high N and 0.34 d^{-1} on medium N), this reduction in A_x must be due mainly to a diminished enlargement of a given population of cells that were generated during the previous exponential phase of leaf growth. By contrast, rate of appearance of new leaves is affected by N supply, due probably to a slower initiation, so that phyllochron

Table 6.6 Leaf response to N and P nutrition in Gmelina arborea *shows that N supply had a strong effect on final size (A_x), with moderate effect on relative rate of expansion (r), whereas P supply impacted principally on r and phyllochron (Δt_0)*

Nutrient treatment	Leaf [nutr]*	Final size A_x (cm^2)	RGR (leaf) r (d^{-1})	Phyllochron Δt_0 (d)
High N	2.94	168	0.36	4.9
Med N	1.18	92	0.34	7.4
Low N	0.63	29	0.24	9.8
High P	0.103	113	0.23	8.5
Med P	0.052	107	0.19	11.2
Low P	0.029	12	0.12	18.9

(Adapted from Cromer *et al.* 1993)

*[nutr] refers to leaf [N] or leaf [P] as mmol N or P g^{-1} dry mass for N and P experiments respectively. A_x and r refer to node 6 in both experiments, and Δt_0 from node 6 to node 7.

(Δt_0 in Table 6.6) increased from 4.9 to 7.4 to 9.8 d on high, medium and low N supply respectively.

Phosphorus effects on leaf growth in *G. arborea* are amenable to a similar analysis. In this case, A_x was less sensitive to reduction from high P to medium P, whereas r was reduced from 0.23 to 0.19 d^{-1} (and to 0.12 d^{-1} on low P). Phyllochron was similarly sensitive, and as with N effects, Δt_0 became protracted with reduction in P supply (namely 8.5, 11.2 and 18.9 d on high, medium and low P respectively). These plants were taking twice as long to produce new leaves on low P as on low N.

In keeping with common experience on a wide range of plants, nutrient deficiency slowed canopy development in *G. arborea*, but present analysis has shown that N and P effects are qualitatively different. N deficiency is obvious as a reduction in leaf size, whereas P deficiency impacts to a relatively greater extent on leaf number due to slower appearance. Moderately N deficient plants (leaf [N] *c.* 1.2 mmol N g^{-1} dry mass) produced a slower succession of smaller leaves that expanded reasonably quickly, but moderately P deficient plants (leaf [P] *c.* 50 μmol P g^{-1} dry mass) produced even fewer leaves (longer phyllochron) that expanded slowly but nevertheless achieved reasonable size. Relative rate of leaf expansion (r) was not different on high N cf. moderate N (r = 0.36 ± 0.03 and 0.34 ± 0.04 respectively) but r was different on high P cf. moderate P (r = 0.228 ± 0.005 and 0.192 ± 0.008 respectively). In the same experiment on *G. arborea*, Cromer *et al.* 1993 (their Figure 7) show dose response curves for r with N saturation ≥ 1.5 mmol N g^{-1} dry mass and P saturation ≥ 100 μmol P g^{-1} dry mass.

N, P and K are highly mobile nutrient elements, and even on well-nourished plants individual leaves show considerable nutrient turnover as older (full size) leaves help furnish nutrient requirements of younger expanding leaves at higher nodes. For example, Hopkinson (1964) provided a detailed P budget for cucumber foliage showing a strong import (up to 0.6 mg P $leaf^{-1}$ d^{-1}) that coincided with rapid expansion, followed by a steady net export (up to 0.15 mg P $leaf^{-1}$ d^{-1}) in response to the P demands of expanding leaves at higher nodes. The time-course of post-maturation senescence will vary according to the overall balance between nutrient supply and demand which depends in turn on root-zone nutrient availability versus requirements for continuing growth and development of new organs.

Where nutrient supply is restricted, turnover in mature leaves will accelerate (especially in fast-growing species) and senescence will hasten — a common feature under N, P or K deficiency (Chapter 16). Conversely, when such nutrient-deficient plants are restored to full supply, leaf growth response can be dramatic (Figure 6.12) with sharp reduction in phyllochron (from 21.4 to 6.2 d in this example) and major increase in A_x (from 65 to 181 cm^2 at node 9; see Table 3 in Cromer *et al.* 1993).

Growth responses to nutrient supply are usually unmistakable, even spectacular (Figure 6.12) and commonly referenced

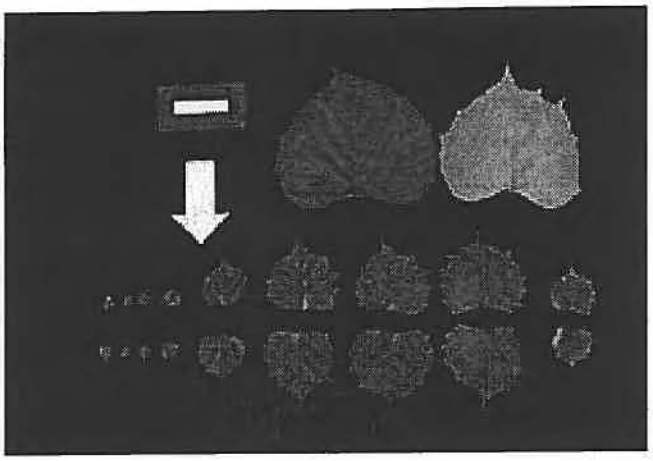

Figure 6.12 *Gmelina arborea* (a relative of teak) is a highly productive tropical tree with large leaves and is favoured as a plantation species. Leaf growth is especially responsive to a step-up from low to medium P supply (subsequent to leaf appearance at node 4, arrow). Relative rate of leaf expansion (r) increased from 0.134 to 0.228 d^{-1}, and phyllochron (Δt_0) decreased from 21.4 to 6.2 d. Upper row shows comparative size of leaves from node 6 on two high-P plants. (Scale bar = 10 cm). (Further details in Cromer *et al.* 1993) (Original photograph courtesy P. E. Kriedemann)

to nutrient element concentration (e.g. [N] or [P]) on a dry mass basis. However, given the highly dynamic nature of tissue N and P, especially when growth-limiting supply enhances recycling from older organs to new growing points, how meaningful are whole-plant or even leaf values for [N] or [P] as driving variables in growth analysis? In effect, [N] and [P] will vary in both space and time according to patterns of plant growth and development, which are themselves influenced by nutrient supply.

Analysis of nutrient-dependent changes in growth indices therefore require test plants where nutrient element concentration can be 'set' in space, and also remain stable in time. These prerequisites can be met by aeroponic culture in a constant environment (see Ingestad and Lund 1986 and literature cited). Seedlings are held in aeroponic spray chambers where a small volume of nutrient solution is recirculated continuously, and further nutrients are introduced at a predetermined relative addition rate (RAR). In effect, a steady exponential growth is set by the RAR of a key nutrient (N or P in present examples, but K is equally amenable) while all other essential nutrients are kept non-limiting. RAR thus represents a driving variable for RGR which in turn shows an initially linear response to RAR (Figure 6.13) eventually reaching a point of saturation (not shown here).

Within a plant's dynamic range of growth response to nutrient supply, RGR and RAR are linearly related so that plants grown this way are well suited to growth analysis. Moreover, whole-plant concentrations of critical nutrients are 'set' by RAR such that higher RAR produces higher whole-plant nutrient concentration and remain reasonably stable over time. Cromer and Jarvis (1990) demonstrated this for N in *Eucalyptus grandis* and Kirschbaum (1991) for P.

Using this Ingestad technique, growth and photosynthetic responses to plant-nutrient concentration are not complicated by interactions between ontogeny and nutrient recycling

discussed earlier. For example, RGR response to plant [N] (Figure 6.14) can now be resolved into NAR and LAR contributions. Taking data from Cromer and Jarvis (1990) for comparisons (cf. Figure 6.13) their highest RAR_N 0.12 d^{-1}, resulted in an RGR of 0.111 d^{-1}, while their lowest RAR_N, 0.04 d^{-1}, generated an RGR of only 0.039 d^{-1}. Corresponding plant [N] values were 34.1 and 11.7 g N kg^{-1} dry mass, and resultant values for NAR were 5.55 and 4.45 g m^{-2} d^{-1} respectively. Higher [N] thus increased NAR by a factor of 1.247. Leaf weight ratio (LWR) increase was somewhat larger (factor of 1.463) and was accompanied by increased SLA (factor of 1.561).

Combining outcomes from Cromer and Jarvis (1990) with those from P experiments by Kirschbaum *et al.* (1992), some key differences between N and P in their effects on growth indices in seedlings of *E. grandis* were apparent. Cromer and Jarvis (1990) concluded, *inter alia*, that '...effects of N on allocation of dry matter to leaves and the way in which dry matter is distributed to intercept light, have a larger influence on seedling growth rate than do effects of N on net rate of carbon gain per unit leaf area'. By contrast, when considering P-dependent effects on RGR, Kirschbaum *et al.* (1992) conclude that '...Carbon fixation rate per unit of plant dry weight increased about 5-fold with increasing nutrient addition rate over the range of addition rates used. That increase was due to a doubling in specific leaf area and a doubling in assimilation rate per unit leaf area, while leaf weight as a fraction of total plant weight increased by about 20 %.' Unlike N, effects of P on RGR were due more to changes in leaf physiology than to changes in dry matter distribution.

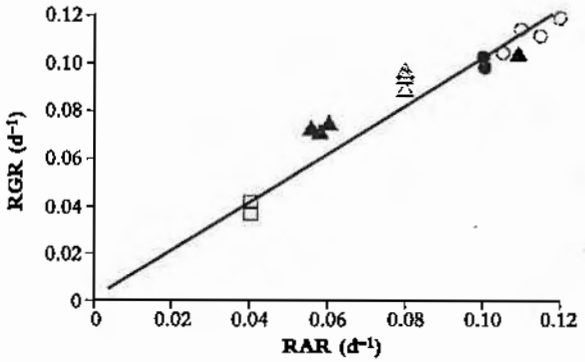

Figure 6.13 RGR of young seedlings (*Eucalyptus grandis*) in aeroponic culture (see Ingestad and Lund 1986 for details on technique) can be set by the relative addition rate (RAR) of a single limiting nutrient (N in this experiment, with all other nutrient elements non-limiting). Clusters of symbols refer to five different RARs, namely 0.04, 0.06, 0.08, 0.10 and 0.12 d^{-1} (with some minor variation)
(Based on Cromer and Jarvis 1990)

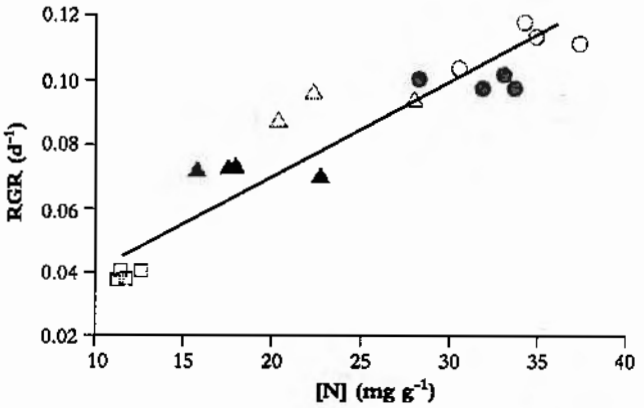

Figure 6.14 Under stable environmental conditions RGR of young seedlings (*Eucalyptus grandis*) growing in aeroponic culture can be set by the relative addition rate (RAR) of a single limiting nutrient (N in this experiment). If exponential growth is maintained, plant-N concentration [N] will be proportional to RAR, and RGR is then linearly related to [N]
(Based on Cromer and Jarvis 1990)

6.2.5 Light × nutrients

Light and nutrients are not only prerequisites for growth, but show a positive interaction in their effect on growth indices. Plant biomass formed per unit plant nutrient (plant-nutrient productivity) increases with irradiance. Birch seedlings grown in aeroponic units under 24 h illumination and constant environment at Uppsala (Figure 6.15a) and *Eucalyptus grandis*

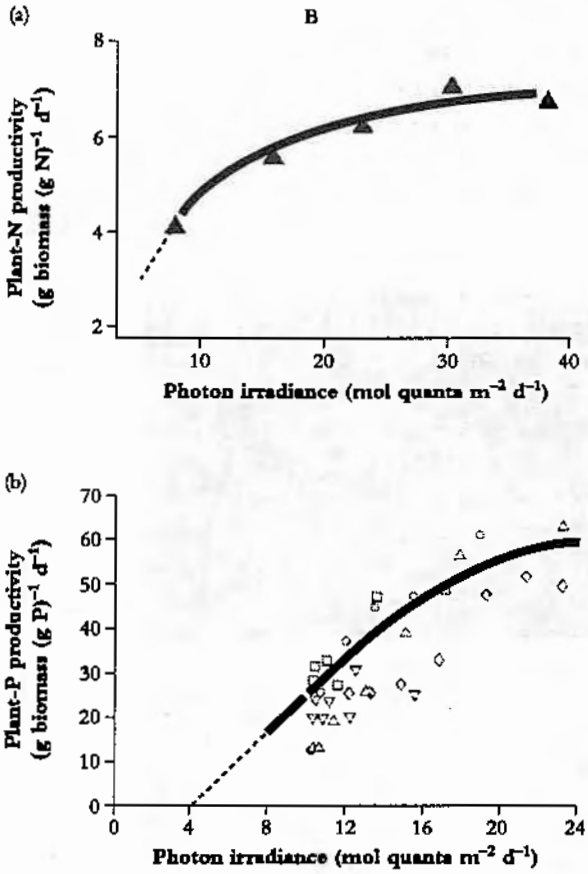

Figure 6.15 Plant-nutrient productivity (biomass formed per unit plant nutrient per unit time) can be inferred from analysis of plants grown in aeroponic culture, and varies with daily irradiance. In (a), plant-N productivity of birch seedlings (*Betula pendula*) grown under continuous illumination in cabinets was saturated around 30 MJ m^{-2} d^{-1}. In (b), plant-P productivity of *Eucalyptus grandis* seedlings in naturally illuminated phytotron cabinets remained unsaturated up to 24 MJ m^{-2} d^{-1}
((a) Based on Ingestad and McDonald 1989, (b) Kirschbaum 1991)

seedlings in Ingestad units under natural light (Figure 6.15b) provide examples of light effects on N and P productivity. In both cases, nutrient productivity has been calculated in terms of whole-plant biomass formed per day per unit plant N or plant P.

Recall from Equation 6.6 that NAR = $(1/A)$ (dw/dt) =s productivity per unit area. In that case, carbon assimilation (biomass gain) was referenced to leaf area per plant. By analogy, nutrient productivity can be referenced to N or P content per plant, so that nitrogen productivity (designated NAR_N) would be

$$NAR_N = \frac{1}{N}\frac{dW}{dt} = \frac{1}{W}\frac{dW}{dt} \times \frac{W}{N} = \frac{RGR}{[N]} \quad (6.15)$$

Similarly, phosphorus productivity (NARP) would be

$$NAR_P = \frac{1}{P}\frac{dW}{dt} = \frac{1}{W}\frac{dW}{dt} \times \frac{W}{P} = \frac{RGR}{[P]} \quad (6.16)$$

Both indices are integrated over successive harvests as with NAR_A, and the same caveats apply, namely both whole-plant biomass and nutrient element content must be increasing exponentially so that a linear relationship exists between whole-plant biomass (W) and plant content of N or P. Leaf-N productivity and leaf-P productivity (i.e. whole-plant biomass increase per unit leaf N or leaf P per unit time) can be derived in the same way.

Plant-N productivity from birch seedlings increases with photon irradiance and approaches an asymptote around 30 mol quanta m^{-2} d^{-1} (Figure 6.15a). Plant-P productivity from *E. grandis* seedlings (Figure 6.15b) can be described by a linear function to *c.* 24 mol quanta m^{-2} d^{-1} and returns numeric values an order of magnitude higher, reflecting the contrasting requirements of these two nutrient elements (Chapter 16). Corresponding estimates of NAR_N and NAR_P on a leaf basis can be used as parameters in process-based models of plant growth where canopy assimilation (and hence biomass gain) is simulated from data on canopy light climate and nutrient concentration in leaves (see Sands 1996 and literature cited).

6.2.6 CO_2 × nutrients

CO_2 is a further prerequisite for growth, and also shows a positive interaction with nutrient supply on plant-growth indices. CO_2 effects on NAR which translate to faster RGR have been documented (Section 6.2.3). Initially strong responses that diminised over time were attributed to a shift in allocation of photoassimilate under elevated CO_2 which resulted in reduced LAR, due in part to decreased SLA plus increased root mass relative to shoot mass in some cases. Photosynthetic acclimation to elevated CO_2 was an additional factor restricting NAR (hence lower RGR), especially on low-nutrient supply. A positive interaction between CO_2 and nutrient supply on NAR would be expected and if nutrient input drives leaf expansion to the extent demonstrated earlier (Section 6.2.4) then the combined effects of LAR × NAR on RGR will be compounded.

Using CO_2 and N supply as driving variables, Wong *et al.* (1992) tested these ideas on seedlings of four species of

Figure 6.16 Growth of *Eucalyptus camaldulensis* (cultured 90 d in unshaded greenhouses) shows a positive and interactive response to factorial combination of N supply and CO_2 (1.2 or 6.0 mM nitrate with 330 or 660 ppm CO_2). Treatments left to right are: low N + low CO_2, high N + low CO_2, low N + high CO_2 and high N + high CO_2. (Scale bar = 50 mm). (Further details in Wong *et al.* 1992)
(Original photograph courtesy P. E. Kriedemann)

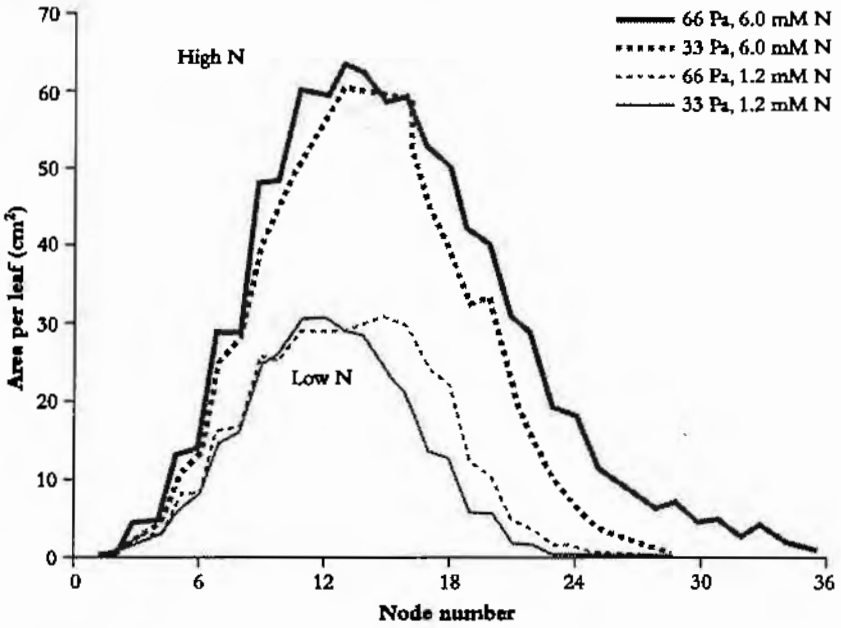

Figure 6.17 Overall growth of *Eucalyptus camaldulensis* showed a strong positive response to CO_2 × N (see Figure 6.16). However, mean area per leaf at each node depended mainly on N supply, showing no consistent interaction with CO_2. In contrast, the number of nodes was increased by CO_2, so that plants were taller and carried more leaves. N and CO_2 were supplied in a 2 × 2 factorial combination of 1.2 or 6.0 mM nitrate with 330 or 660 ppm CO_2) for 90 d in unshaded greenhouses
(Based on Wong *et al.* 1992)

eucalypt which represented ecologically distinctive groups, namely *Eucalytus camaldulensis* and *E. cypellocarpa* (both fast growing, widely distributed and reaching immense size) versus *E. pulverulenta* and *E. pauciflora* (more limited distribution, smaller final size and restricted to poor sites). In addition, two subgenera were represented: *E. camaldulensis*, *E. cypellocarpa* and *E. pulverulenta* belong to the subgenus *Symphyomyrtus*, whereas *E. pauciflora* belongs to *Monocalyptus*. Systematic differences between subgenera in physiological attributes have been noted (Noble 1989). According to that scheme, *E. pauciflora* would show more muted response to CO_2 × nutrient inputs compared with the other three species.

In Wong *et al.* (1992) early exponential growth showed a strong response to CO_2 × N treatments where CO_2-dependent increase in RGR (ΔRGR) was clearly influenced by N supply. All three *Symphyomyrtus* species returned a greater ΔRGR on high N. By contrast, the *Monocalyptus* species *E. pauciflora* showed no such CO_2 × N interaction.

Given the scale of CO_2 × N effects on canopy growth (Figure 6.16, and Table 7 in Wong *et al.* 1992), *E. camaldulensis* was taken for more detailed analysis at final harvest (Figure 6.17). CO_2-enriched plants on high N were clearly tallest and carried the largest canopies (Figure 6.16) but maximum area per leaf (around node 12 in Figure 6.17) was driven by N rather than CO_2. Nutrient impact on leaf expansion is well known (Section 6.2.4), and present effects are consistent with those general responses. Accordingly, CO_2 × N interaction on canopy area of *E. camaldulensis* can be attributed to stem extension and generation of leaf number (CO_2 effect at high N), as well as greater size per leaf (nutrient effect and independent of CO_2).

Leaf function is also reflected in leaf-N productivity (whole-plant dry mass formed per unit leaf N per day; Table 6.7). Species differences are again evident where *E. camaldulensis* and *E. cypellocarpo* were decidedly higher while *E. pulverulenta* and *E. pauciflora* what somewhat lower. In addition, elevated CO_2 increased leaf-N productivity for both *E. camaldulensis* and *E. cypellocarpa* on either high N or low N, whereas the other two species *E. pulverulenta* and *E. pauciflora* varied in scale and direction. Indeed, high N may have proved supraoptimal for those two species, and especially in combination with high CO_2.

Table 6.7 Leaf-N productivity (leaf-N-use efficiency for whole-plant growth) in eucalypt seedlings varies as a function of CO_2 and N supply, but with contrasts between species that relate to source habitat

CO_2 (ppm)	N supply (mM)	Leaf-N productivity (g dm (mol N)$^{-1}$ d^{-1}) Sp. 1	Sp. 2	Sp. 3	Sp. 4
330	1.2	102.9	100.7	63.3	52.9
330	6.0	85.8	94.2	52.6	88.1
660	1.2	162.1	127.7	85.4	83.8
660	6.0	112.5	136.6	38.8	78.3

(Adapted from Wong *et al.* 1992)
Species 1, *Eucalytus camaldulensis*; species 2, *E. cypellocarpa*; species 3, *E. pulverulenta*; species 4, *E. pauciflora*.

Leaf N is ultimately responsible for carbon gain, so that NAR and leaf-N productivity are functionally related. In those species adapted to fast capture of nutrient-rich sites such as *E. camaldulensis* and *E. cypellocarpa* a capacity for high NAR based upon efficient use of leaf N (i.e. high leaf-N productivity) would confer a selective advantage. By contrast, *E. pulverulenta* and *E. pauciflora* were collected from resource-poor sites where fast growth would have been selectively neutral.

6.2.7 Water

Growth is a turgor-dependent process, and later phases of leaf expansion that depend principally upon cell enlargement are especially sensitive to water stress. When plants encounter water stress, leaf area increase is either diminished or even ceases well ahead of any clear reduction in leaf gas exchange. NAR is thus less sensitive to water stress than RGR_A, a distinction reported as early as 1943 for greenhouse tobacco plants at the Waite Institute. In a posthumous paper compiled by JG Wood, Petrie and Arthur (1943) subjected tobacco to four watering treatments, namely high-water range, low-water range, early temporary drought and late temporary drought. Growth indices were derived from nine sequential harvests and plant biomass analysed for total N, protein N, soluble sugars and crude fibre. NAR was expressed in terms of area, mass and protein content of leaves.

Total plant biomass at final harvest was greatly reduced by the low-water treatment due largely to early reductions in leaf expansion. NAR (area basis) was not affected to the same extent as final biomass but NAR ('protein' basis) was substantially reduced because leaf 'protein' was increased by water stress.

Especially significant, and perhaps paradoxically, JG Wood reported that 'Both early and temporary drought cause an initial depression in growth rate due to a depression in net assimilation rate; this is followed by an increase in growth rate greater than that of the high-water plants. This increase is due to the greater protein content of the plants subjected to temporary drought.' A single cycle of early drought and subsequent recovery resulted in whole-plant RGR that was still comparable to non-stressed controls. Since NAR (area basis) was relatively insensitive, significant reduction in final biomass must have been due to an initial reduction in leaf growth.

Early temporary drought (applied from day 64 to day 81 in a growing season of 175 d) enhanced growth of both shoots and roots subsequent to stress relief (rewatering). Total leaf area at 118 days was 7000 cm^2 following early drought, compared with 5300 cm^2 in unstressed controls, so that final size per leaf on upper nodes must have been considerably greater. A build up of 'protein' during drought was thought to have boosted expansion of later-formed leaves subsequent to rewatering, but in retrospect, accumulation of osmotically active materials during drought stress was almost certainly an

added factor in this compensatory growth. For example, some sunflower cultivars respond to drought stress and recovery cycles by generating individual leaves that are as much as 60% larger than leaves on corresponding nodes of unstressed controls (Rawson and Turner 1982). Leaf-growth dynamics that underlie such a remarkable response are discussed below and are based on some earlier studies of Takami *et al.* (1981).

Takami *et al.* (1981) grew sunflowers in a greenhouse under natural light in Canberra (March–May 1980). Seedlings were initially well watered to ensure good establishment (first 15 d). After thinning to two plants per pot, irrigation was then withheld from some pots, and unstressed controls were maintained near field capacity. Drought stress developed slowly (as intended) and drought-stressed plants recovered fully within 4–6 d of irrigation. Just prior to rewatering, pre-dawn leaf turgor was actually higher in stressed plants (0.63 MPa) compared with controls (0.39) notwithstanding a rather lower bulk leaf water potential (Ψ_{leaf} = –0.47 and –0.16 MPa in stressed and control respectively).

Leaf-growth dynamics (Table 6.8) are based on comparisons between mean data for control and stress-recovered plants, and apply to corresponding nodes, namely 5, 13, 17 and 23. Final leaf size varies with node number in sunflower (Figure 6.7) hence the need for strict correspondence. Leaves at node 5 (Table 6.8) encountered an intensifying stress soon after appearance. Stressed plants maintained similar r, and failed to reach the same final size (A_x) as well-watered controls. Taking r as indicative of cell division during the exponential phase of lamina expansion with subsequent growth driven mainly by enlargement, drought stress has restricted cell enlargement rather than cell division.

Leaves at node 13 on droughted plants (prior to stress relief on day 36) were similar in RGR (r = 0.24 d^{-1} cf. 0.26 d^{-1} in well-watered controls) but greatly restricted in final size (84 cm^2 cf. 392 cm^2 in controls), again emphasising the sensitivity of cell enlargement to moisture stress.

Table 6.8 Moisture stress in pot-grown Helianthus annuus *slowed emergence of new leaves and reduced their final size but with little effect on RGR of individual leaves (r). This outcome implies that later stages of leaf expansion (where cell enlargement rather than cell division predominates) are especially sensitive to water supply. Similarly, rewatering has little effect on r, but took effect by node 23 where Δt_0 is reduced and final size (A_x) is increased substantially compared with well-watered controls*

Treatment	Node	Final size A_x (cm^2)	RGR (leaf) r (d^{-1})	Phyllochron Δt_0 (d)
Watered	5	186	0.26	—
Stressed	5	154	0.28	—
Watered	13	392	0.26	1.4
Stressed	13	84	0.24	1.2
Watered	17	314	0.22	1.4
Post-stress	17	253	0.20	3.2
Watered	23	198	0.18	1.1
Post-stress	23	228	0.19	0.8

(Adapted from Takami et al. 1981)

Phyllochron (Δt_0 in Equation 6.14) was little affected up to node 13 (Table 6.8) but after-effects of previous stress became apparent on rate of leaf appearance from node 14 to node 17, resulting in Δt_0 increasing from 1.4 to 3.2 d. Subsequent leaf appearance (node 17 to node 23) was even accelerated in stress-recovered plants, resulting in a Δt_0 = 0.8 d cf. 1.1 d in non-stressed controls. r at node 23 was unchanged by stress-recovery treatments but final size was substantially greater (228 cm^2) in stress-recovered compared with non-stressed controls (198 cm^2). Such compensatory growth by individual leaves following stress relief would draw on N-based resources that accumulate during drought, while turgor-driven expansion to a greater final size would be a consequence of drought-induced osmotic adjustment.

6.3 Developmental physiology

Growth is an irreversible increase in plant size accompanied by a *quantitative* change in biomass. Development is more subtle and implies an additional *qualitative* change in plant form or function. Development thus lends 'direction' to growth and can apply equally well to a progressive change in gross morphology as to a subtle change in organ function, or to a major phase change from vegetative to reproductive development.

In all cases, resource utilisation and photoassimilate partitioning will be affected by growth and development with consequences for reproductive success in nature or utility in managed crops. Such outcomes are amenable to quantitative analysis.

6.3.1 Biomass distribution

Roots and shoots are functionally interdependent and these two systems maintain a dynamic balance in biomass which reflects relative abundance of above-ground resources (light and CO_2) compared with root-zone resources (water and nutrients). Whole-plant growth rate and root:shoot ratio are thus an outcome of genotype × environment interaction, but source of control is ambiguous.

According to one argument, internal (genetic) control over root:shoot ratio will be expressed throughout growth and development and will thus dictate resource capture both above and below ground, and hence whole-plant growth rate. Change in root:shoot ratio during a plant's life cycle is then regarded as part of a gene-controlled ontogeny. An alternative view, and well supported by observation, is that growth rates of roots and shoots continually adjust in response to resource capture with photoassimilate (hence biomass) allocated on a 'needs basis'.

In practice, both models apply because developmental morphology is ultimately gene dependent but expression of a

given genotype will vary in response to growing conditions (hence phenotypic plasticity).

Irradiance is a case in point where shoot growth takes priority in low light, whereas root growth can be favoured under strong light. For example, Evans and Hughes (1961) grew *Impatiens parviflora* at five light levels and demonstrated a steady increase in root mass relative to whole-plant mass (root mass ratio) from 7% to 100% full sun. Stem mass ratio showed the opposite sequence. Leaf mass ratio increased somewhat at low light, but increased SLA was far more important for maintenance of whole-plant RGR in this shade-adapted species (discussed earlier in connection with Table 6.2).

If light effects on root:shoot ratio are translated via photosynthesis, then CO_2 should interact with irradiance on root:shoot ratio because carbon assimilation would be maintained by a more modest investment in shoots exposed to elevated CO_2. *Chrysanthemum morifolium* behaved this way for Hughes and Cockshull (1971), returning a higher NAR due to CO_2 enrichment under growth cabinet conditions despite lower LAR which was in turn due to smaller leaf weight ratio. Adjustment in SLA exceeded that of leaf weight ratio, and so carried more significance for growth responses to irradiance × CO_2.

In parallel with shoot response to above-ground conditions, root biomass is influenced by below-ground conditions where low availability of either water or nutrients commouly leads to greater root:shoot ratio. For example, inoculated white clover (*Trifolium repens*) growing on a phosphorus -rich medium increased root:shoot ratio from 0.39 to 0.47 in response to moisture stress; and from 0.31 to 0.52 when moisture stress was imposed in combination with lower phosphorus (see Table 1 in Davidson 1969). A positive interaction between low phosphorus and low water on root:shoot ratio was also evident in perennial ryegrass (*Lolium perenne*) grown on high nitrogen. In that case, root:shoot ratio increased from 0.82 to 3.44 in response to moisture stress when plants were grown on low phosphorus in combination with high nitrogen.

Adding to this nutrient × drought interaction, a genotype × phosphorus effect on root:shoot ratio has been demonstrated by Chapin *et al.* (1989) for wild and cultivated species of *Hordeum*. Weedy barleygrass (*H. leporinum* and *H. glaucum*) was especially responsive, root:shoot ratio increasing from about 0.75 to 1.5 over 21 d on low phosphorus. By contrast, cultivated barley (*H. vulgare*) remained between 0.5 and 0.75 over this same period. Held on high phosphorus, all species expressed comparable root:shoot ratios which declined from around 0.55 to about 0.35 over 21 d. High root:shoot ratios on low phosphorus in weedy accessions would have conferred a selective advantage for whole-plant growth under those conditions, thus contributing to their success as weeds.

Even stronger responses to phosphorus nutrition have been reported for soybean (Fredeen *et al.* 1989) where plants on low phosphorus (10 μM KH_2PO_4) invested biomass almost equally between roots and shoots, whereas plants on high phosphorus (200 μM KH_2PO_4) invested almost five times more biomass in shoots than in roots (daily irradiance was *c.* 30 mol quanta m^{-2} d^{-1} and would have been conducive to rapid growth).

Root:shoot ratios are thus indicative of plant response to growing conditions, but by their very nature ratios are not a definitive measure because values change as plants grow. In herbaceous plants, root:shoot ratios typically decrease with age (size) due to sustained investment of carbon in above-ground structures (root crops would be a notable exception). Trees in a plantation forest would also show a progressive reduction in root:shoot ratio, and especially after canopy closure where a steady increase in stem biomass contrasts with biomass turnover of canopy and roots and thus predominates in determining root:shoot ratio.

Meaningful comparisons of root:shoot ratio must therefore be referenced to whole-plant biomass and some examples cited by Bastow Wilson (1988) meet this criterion, and in so doing exclude ontogenetic effects. Broad generalisations coincide with examples cited above, namely root:shoot ratio increases with nutrient deficiency and moisture stress or under elevated CO_2, but decreases in strong light. Too often, however, reports of treatment effects on root:shoot ratio can be artefacts of contrasts in whole-plant biomass. Equally, some real responses may be obscured. Allometry then becomes a preferred alternative where repeated measurements of size or mass provide an unambiguous picture of carbon allocation.

Allometry

During whole-plant growth in a stable environment, roots and shoots maintain a dynamic balance such that

$$y = bx^k \tag{6.17}$$

where y is root biomass and x is shoot biomass. More generally, x and y can be any two parts of the same organism that are growing differentially with respect to each other, but root–shoot relations are the most common candidate in such analyses of plant growth.

The allometric equation $y = b.x^k$ (Equation 6.17) can be ln transformed to become

$$\ln y = \ln b + k \ln x \tag{6.18}$$

This formulation enables a straight-line plot of ln y as a function of ln x with slope k (i.e. the allometric coefficient) and intercept ln b. This empirical model does not explain the nature of growth controls between roots and shoots but does offer a simple description which is not confounded by plant size. Moreover, any departure from a particular root:shoot relationship is immediately obvious, and sources of variation in root:shoot ratio can be resolved into starting conditions (differences in intercept, ln b) versus biomass partitioning during growth (differences in slope, k).

Leaf, stem and root growth under controlled conditions in *Eucalyptus grandis* seedlings demonstrate such application

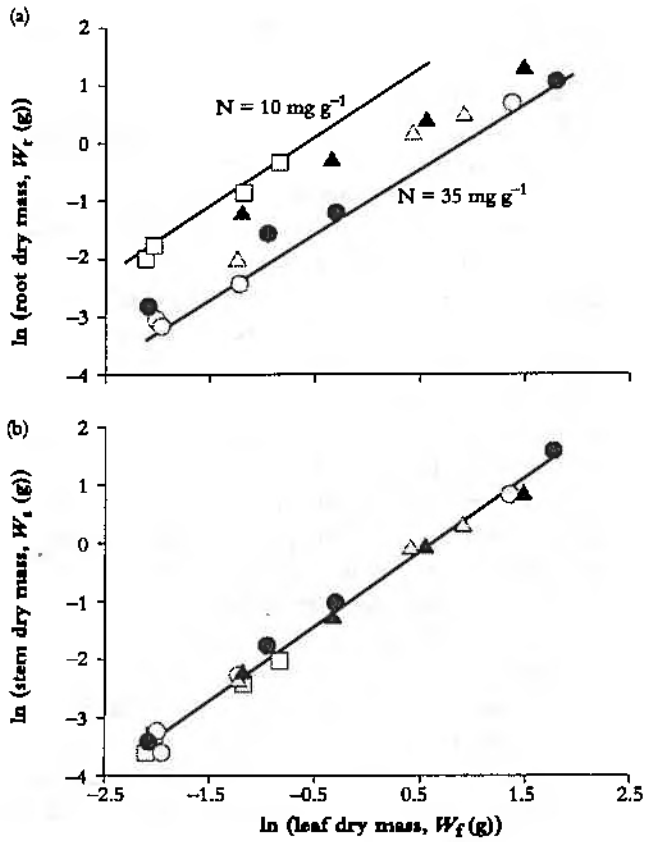

Figure 6.18 Seedlings of *Eucalyptus grandis* growing in aeroponic culture on five different nitrogen treatments show a strict allometry between root (W_r) and leaf growth (W_f) (a) as well as between stem (W_s) and leaf growth (b). With all other nutrient elements non-limiting, nitrogen was supplied at five relative addition rates (d^{-1}), namely 0.12 (open circle), 0.10 (solid circle), 0.08 (open triangle), 0.06 (solid triangle) and 0.04 (open square). Root:leaf allometry in seedlings on the lowest RAR_N (plant [N] 10 mg g^{-1}) shows a similar slope but a higher intercept compared with plants maintained continuously on the highest RAR_N (plant [N] 35 mg g^{-1}). Stem:leaf allometry (b) was highly conserved regardless of RARN with a slope (k) of 1.261 reflecting a steady commitment to stem growth over leaf growth in these tree seedlings (Based on Cromer and Jarvis 1990)

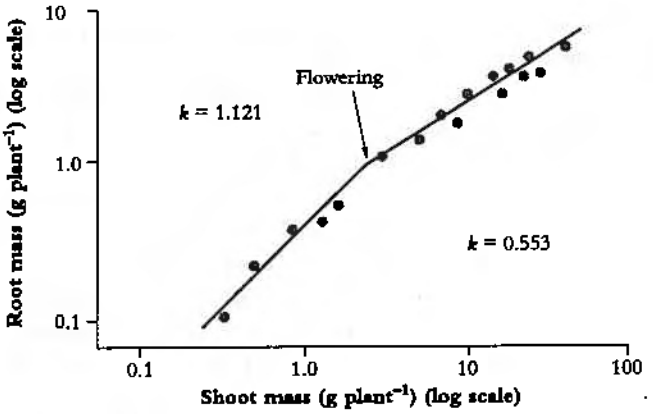

Figure 6.19 Root:shoot allometry in Italian ryegrass (*Lolium multiflorum*) shows an abrupt change with flowering (log–log plot). A change in allometric coefficient (k) for this species from 1.121 to 0.553 indicates a shift in biomass allocation from root growth towards shoot growth following emergence of inflorescences. Mean values for k during vegetative cf. reproductive phase from several accompanying species were 1.145 and 0.627 respectively (Based on Troughton 1956)

(Figure 6.18a,b; Cromer and Jarvis 1990). Nitrogen input in nutrient spray chambers was used as a driving variable for growth where five relative addition rates (RAR_N) generated a wide range in whole-plant RGR (from 0.039 d^{-1} on lowest RAR_N to 0.111 d^{-1} on highest RAR_N).

Data from all treatments and harvests were pooled to reveal a strict allometric relationship between root and leaf growth (Figure 6.18a) with a nitrogen effect on intercept but not slope. Nitrogen nutrition had influenced biomass allocation to the extent that low RAR_N had initially promoted root growth relative to leaves (hence higher intercept), but subsequent to this early adjustment, and once growth had stabilised, biomass allocation to roots and leaves maintained a constant relationship irrespective of RAR_N. In this case k = 0.982, indicating a net bias towards leaf growth over root growth — a 'net bias' because carbon loss via excretion, root renewal and respiration was not measured so that more photoassimilate would have been allocated to roots than was fixed in biomass.

Stem and leaf biomass also maintained a strict allometric relationship (Figure 6.18b) where k = 1.261. A value for k greater than unity implies a consistent bias towards stem growth relative to canopy growth, as would be expected in a eucalypt with a high rate of stem growth (and favoured in plantation forestry). Significantly, nitrogen treatment was without effect on either intercept or slope (Figure 6.18b) and emphasises the highly conserved relationship between leaves and stem in these seedlings.

Developmental events also influence allometry and Italian ryegrass (*Lolium multiflorum*) provides a nice example (Figure 6.19) where a log–log plot of root mass as a function of shoot mass showed an abrupt change in slope when flowering occurred. In that case, k decreased from 1.121 to 0.553, and although shoot dry mass was about 10 times root biomass, a change in allometry was clearly evident.

Allometry is most commonly applied to roots and shoots, but other functional interrelations within plants are equally amenable, and especially where non-destructive measurements are involved. Length and breadth of leaves, or length and circumference of fruits enable calculation of k values that categorise shape, and can reveal heritabilities in developmental morphology. The two variables can even carry different dimensions as in stem volume and leaf area or canopy area and plant mass. In that case, a 'ratio' of area to mass coincides with leaf area ratio (LAR, Section 6.1). Compared with that cumulative but static index, the allometric relationship between canopy area and plant mass (termed 'α' by Whitehead and Myerscough 1962) is a more dynamic indicator of '... the proportion of dry weight increment surplus to that required to maintain the morphogenetic proportions of the plant as an efficient photosynthetic form alone. When α is unity all the dry-weight increment is used up in maintaining the proportions of the plants as a 'photosynthetic entity'...'. Soon after germination, seedlings gain leaf area at the expense of dry

mass and α will be <1.0. Similarly, during latter phases of maturation when leaf area can be decreasing while whole-plant mass is still increasing, α will again be <1.0, and in both cases α is simply reflecting normal ontogenetic drift. However, in a plant community where individuals are competing for light, if α remains <1.0 during that early phase of a plant's lifecycle when both leaf area and plant mass are increasing exponentially, such individuals will fail to survive. Time trends in α can thus be used to predict future performance with respect to biomass gain, or to analyse adjustments in biomass distribution under contrasting environmental conditions.

6.3.2 Size and ontogeny

Vascular plants increase in both size and complexity during vegetative growth and reproductive development, showing changes in growth indices that are characteristic of ontogenetic drift (sensu Evans 1972). Size is a major factor for RGR (Table 6.9). This brief survey of wide-ranging taxa shows how values can range over three orders of magnitude. Single-celled organisms such as bacteria and algae vary between 5 and 20 d^{-1} (corresponding to a doubling time of 0.14 and 0.04 d respectively). By contrast, RGR for young vascular plants including crop species rarely exceeds 0.4 d^{-1} even during early vegetative growth and is more commonly around 0.1 d^{-1}. Particular organs on vascular plants can, however, achieve faster growth and most notably young leaves can double in size every day or so during their first week of (exponential) growth.

With size comes complexity, and especially in vascular plants where specialised tissues constantly differentiate as organs and participate in resource exchange as either sources or sinks. Perennial plants represent an extreme case where biomass accumulates as inert structures and where cycles of differentiation and renewal last years rather than days. Whole-plant RGR is typically lower in these species. For example, Jarvis and Jarvis (1964) cite representative values for birch seedlings growing in nutrient solution of *c.* 0.12 d^{-1} compared with parallel cultures of sunflower of *c.* 0.24 d^{-1}.

Table 6.9 Relative growth rate (d^{-1}) and thus doubling time (d) vary widely according to size and complexity of organisms and their component organs. Unicellular bacteria and algae are typically fast whereas multicellular herbaceous plants take much longer to double their size or dry mass. Perennial plants are even slower due especially to large investments of biomass in structural components and long-term storage

Organism	Relative growth rate (typical range, d^{-1})	Doubling time (d)
Bacteria	5–20	0.14–0.04
Algae (single celled)	1–4	0.69–0.17
Root apices	1–3	0.69–0.23
Stem apices and young leaves	0.3–1.0	2.31–0.69
Germinating embryos	0.2–0.8	3.47–0.87
Crop seedlings and field weeds	0.1–0.4	6.93–1.73
Shade-adapted spp.	0.02–0.04	34.65–17.33
Perennial plants	0.005–0.02	140–35

(Composite data from various sources including Jarvis and Jarvis 1964, Warren Wilson 1972 and Williams 1975)

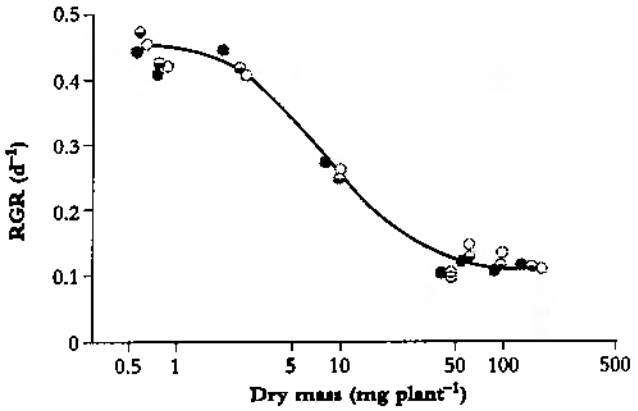

Figure 6.20 RGR for whole plants (g g^{-1} d^{-1}) is size dependent and commonly diminishes as growth and reproductive development proceed (ontogeny). Three lines of a semi-dwarf wheat designated here by three different symbols differ in their complement of dwarfing genes (*Rht*) and thus in final size and absolute growth rate, but when referenced to plant mass there are no intrinsic differences in RGR.
(Based on Bush and Evans 1988)

Even highly selected crop species show an ontogenetic drift in RGR and a semi-log plot of RGR versus plant mass for different wheat genotypes (Figure 6.20) illustrates this principle. Bush and Evans (1988) grew isogenic lines of tall and dwarf wheat in natural light under Canberra phytotron conditions using four day/night temperature regimes in combination with three daylengths (8, 11–12 and 16 h) and with daily irradiance treatments that ranged between *c.* 8 and 25 MJ m^{-2} d^{-1}. A strong genotype × environment interaction on whole-plant growth was evident in their experiment. Tall isogenic lines were consistently larger due to faster and more uniform germination (Figure 2 in Bush and Evans 1988) but whole-plant RGR was similar for both tall and dwarf lines, and when plotted as a function of dry mass (log scale in Figure 6.20) genetic differences disappeared.

Other cases of gene × environment effects on plant growth do embody genetic differences, but once again, contrasts in plant size must be accommodated for valid comparisons of RGR to emerge. For example, Dijkstra and Lambers (1989) grew two subspecies of *Plantago major* (large plantain) in a controlled environment and established a genetic difference between the two subspecies (Figure 6.21). *P. major* L. is an inbreeding perennial that forms a rosette and is distributed world wide. *P. major* ssp. *major* L. is slow growing and late flowering, but withstands stresses such as soil compaction and mowing, and is thus a common weed in lawns and on road sides. By contrast, *P. major* ssp. *pleiosperma* (Pilger) is a fast-growing annual, early flowering and an opportunistic coloniser, producing a great number of small seeds and commonly found on river banks and tilled fields.

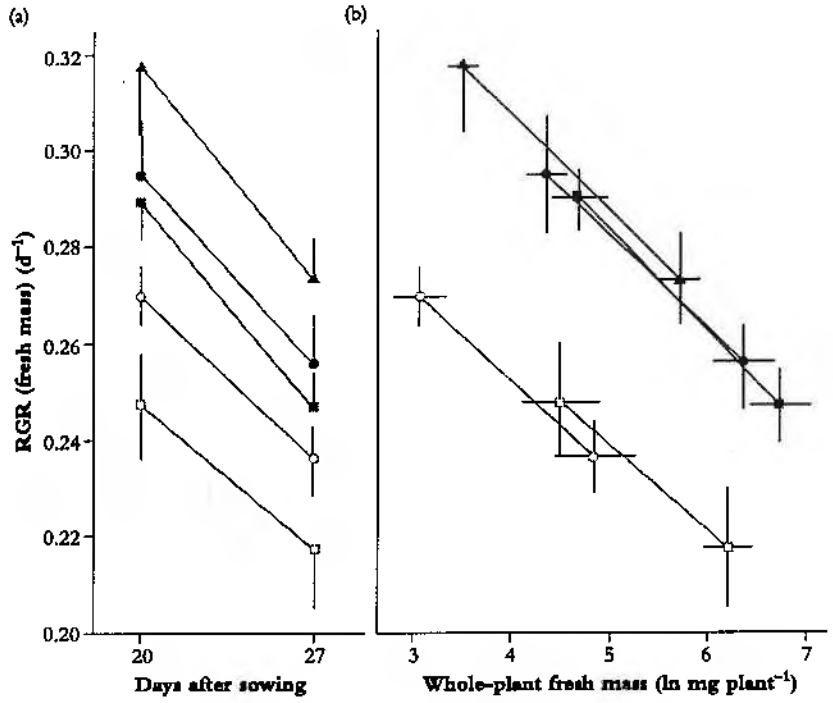

Figure 6.21 Two subspecies of *Plantago major* known to differ with respect to growth rate under natural conditions were raised in a controlled environment (13 mol quanta m^{-2} d^{-1} and 20°C day and night). RGR diminished with age in all cases (a) and genetic differences did not become apparent until data were referenced to plant mass (b). The higher RGR in *P. major* ssp. *pleiosperma* (solid symbols) compared with *P. major* ssp. *major* (open symbols) was associated with higher SLA and lower respiratory losses
(Based on Dijkstra and Lambers 1989)

Both subspecies decreased in RGR with time (Figure 6.21a) regardless of size class, but any clear genetic differences were obscured in these pooled data. However, when RGR data from the two subspecies were plotted as a function of whole-plant fresh mass (Figure 6.21b) age and/or size effects were accommodated and an intrinsic difference in RGR became apparent.

Applying this same rigour in other comparative studies, Dijkstra and Lambers (1989) report intraspecific differences in nutritional physiology, growth response to irradiance, tolerance to trampling and resistance to soil compaction. By eliminating age and/or size as a factor in growth analysis, and thus removing ontogenetic drift as a confounding variable, genotype versus environmental effects on growth indices have been resolved.

6.3.3 Reproductive development

Annual plants show a sigmoidal increase in total biomass during each life cycle (Figure 6.22) where a near-exponential vegetative phase (Phase 1) gives way to a reproductive phase (Phase 2) starting with flower initiation. In effect, Phase 1 sets a potential for reproductive yield whereas events during Phase 2 determine realisation of that potential because nearly all of the photoassimilate stored in reproductive structures (90–95% in cereal grains, for example) comes from carbon fixed subsequent to initiation. Reproductive organs then become dominant sinks for current photoassimilate as well as carbon-based resources previously stored in leaves and stems.

The carbon content of shoot components changes dramatically following onset of reproductive development (e.g.

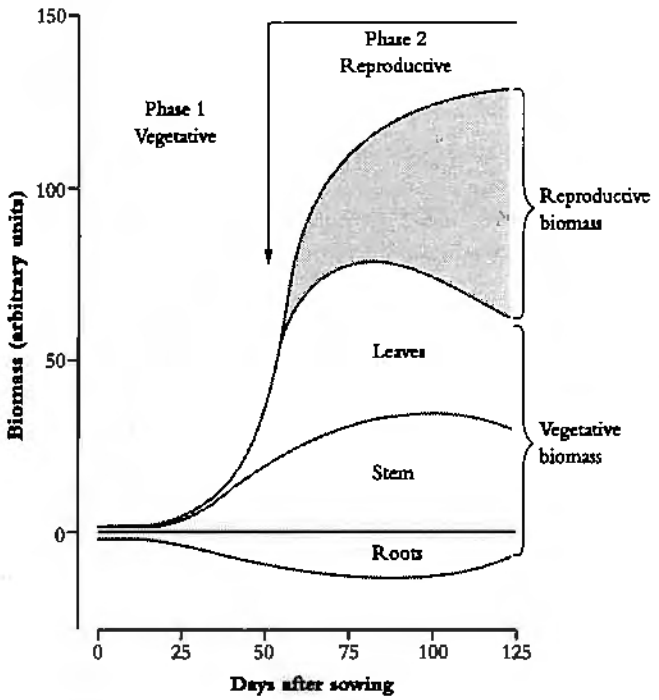

Figure 6.22 A notional distribution of biomass during vegetative growth and reproductive development in an idealised annual plant such as a cereal or grain legume over *c.* 125 d. Whole-plant biomass follows a sigmoidal pattern with a near-exponential increase during vegetative growth and an asymptotic increase during subsequent maturation. Reproductive structures have by then become dominant sinks for photoassimilate, drawing 90–95% of their carbon from current photosynthesis but also mobilising stored assimilate from leaves, stems and roots, which lose biomass during that process

lupin in Figure 6.23) and the dynamic balance between leaves and stem that had been previously maintained during vegetative growth is now replaced by an accelerated senescence of leaves and loss of non-structural carbohydrates from leaves

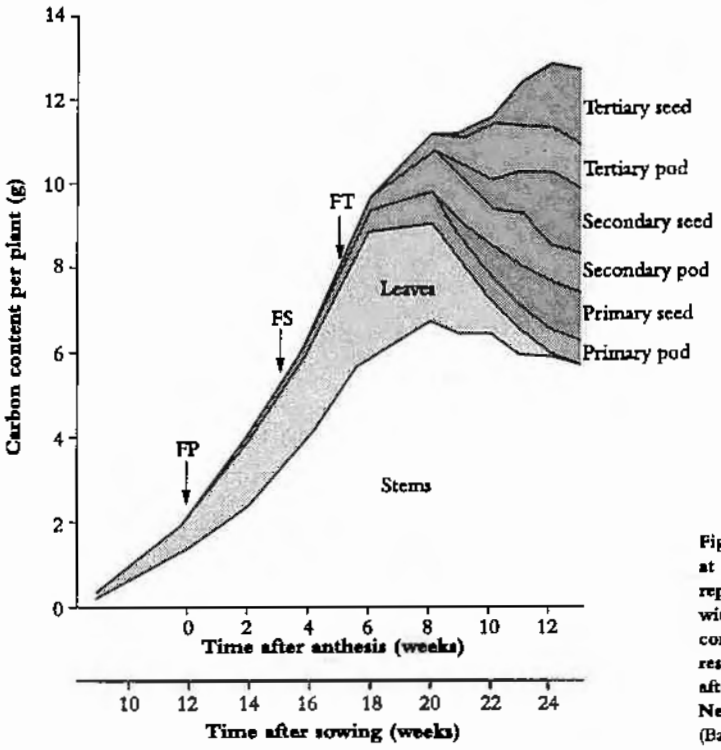

Figure 6.23 An unirrigated crop of lupin (*Lupinus angustifolius* cv. Unicrop) at Perth shows major redistribution of plant carbon from vegetative to reproductive structures during grain filling. This cultivar is indeterminate with successive cycles of reproductive development. FP, FS and FT indicate commencement of flowering on primary, secondary and tertiary shoots respectively. Seed carbon increased exponentially over the period 8–12 weeks after anthesis coinciding with leaf loss and some reduction in stem carbon. Nearby irrigated lupins retained leaves much longer
(Based on Pate *et al.* 1980)

plus stems with a resultant loss in biomass (see also Rawson and Evans 1971). At full maturity (24–25 weeks after sowing in Figure 6.23) reproductive structures account for about 50% of above-ground biomass (represented in that case as plant carbon) with seeds accounting for about two-thirds of that investment). A ratio of harvested biomass to total shoot mass or shoot harvest index (shoot HI, sensu Donald 1962) for these lupin plants was thus about 0.33. Harvest index can apply equally well to the ratio of harvested biomass to total plant biomass (shoots plus roots) but shoot HI is more common in agronomy because root dry mass is so difficult to measure.

In nature, a combination of ecological factors and life cycle options has led to wide variation in reproductive effort by vascular plants so that dry matter invested in reproductive structures relative to vegetative biomass will vary accordingly. For example, late successional rainforest species which combine shade adaptation with longevity are characterised by large propagules where massive seed reserves buffer young seedlings against shortfalls in carbon supply due to deep shade or dry spells. By contrast, early successional (pioneer) species on disturbed sites benefit by producing a large number of widely disseminated seeds. Their reproductive effort is best invested in number rather than size, and carries an added advantage that at least some viable seed will be produced even under stressful conditions. Weedy barleygrass is a case in point where Chapin *et al.* (1989) report that these species produce 4.5-fold more grains, but they are only one-sixth the size of cultivated barley. Ripening patterns also differed where grains matured synchronously in cultivated barley, but matured and dehisced progressively from tip to base in ears of barleygrass.

Domesticated plants have been subjected to sustained selection pressures on reproductive development by humans (Table 6.10) and now reflect wide variation from tuber-forming species such as potato, where over 80% of plant biomass is harvested as storage organs, to high-value flower crops such as tulip where blooms might represent only 20% of the final biomass of whole plants. Mid-range are legumes, cereals and other grain crops where human selection for yield has led to a notable increase in HI. Wheat, for example (Figure 6.24), increased from between 0.30 and 0.35 to almost 0.55 over a century, while barley and rice have shown similar trends. Gifford (1986) documents yield improvement in cereals,

Table 6.10 Harvest index, or HI (dry mass of harvested component/total plant dry mass), varies widely according to crop species and mode of reproduction. Plant breeders select for higher HI as part of crop improvement strategies and have achieved some substantial gains and their higher values are listed here

Crop plant	Harvested component	Harvest index
Potato	Tubers	0.82
Sweet potato	Tubers	0.65
Wheat, barley	Grain	0.55
Maize	Grain	0.52
Peanut	Pods	0.50
Sugar beet	Root	0.50
Rice	Grain	0.50
Sunflower	Seeds	0.50
Chrysanthemum	Flowers	0.46
Cotton	Bolls	0.33
French bean	Pods	0.25
Tulip	Flowers	0.20

(Composite data drawn from a variety of sources including Evans 1975, 1993; Gifford 1986 and Warren Wilson 1969)

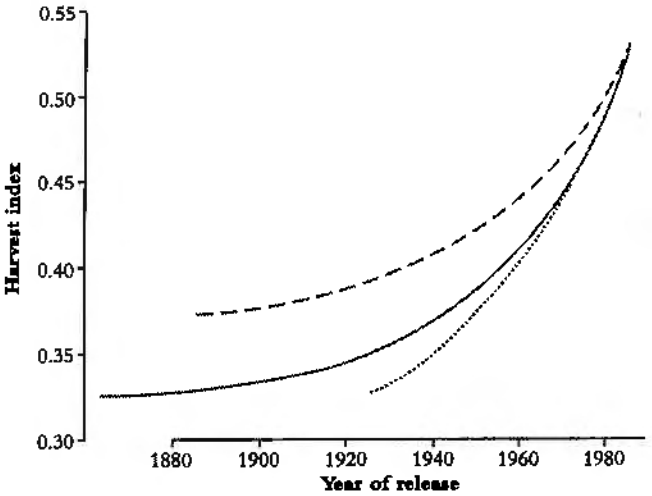

Figure 6.24 A century of breeding and selection has produced some solid gains in harvest index (HI) (ratio of grain to whole-plant biomass) for crop species including barley (dashed line), wheat (solid line) and rice (dotted line) as shown here. Introduction of dwarfing genes to reduce lodging under high-nutrient cultivation was a major factor in this achievement. Cereal architecture necessitates some trade off between stout stems to support heavy ears and a retention of leaf area to generate photoassimilate. HI will eventually reach a ceiling set by those constraints
(Based on Evans 1993)

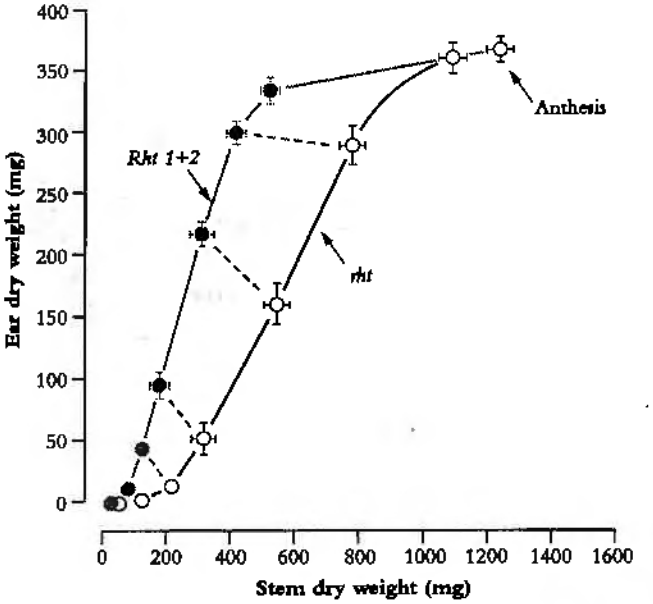

Figure 6.25 Early growth of reproductive tissues relative to stem mass in dwarf genotypes foreshadows faster ear development and higher HI. The tall and productive Mexican spring wheat (Yaqui 50, designated *rht*) eventually produces heavier ears, but returns a lower HI at maturity. Introduction of two major dwarfing genes (*Rht 1* + *Rht 2*, hence *Rht 1 + 2* indicated here) resulted in shorter stems. Consequently, developing ears were subject to less competiton for photoassimilate during early differentiation and for grain filling subsequent to anthesis. Successive (coincident) harvests for these two lines are connected by broken lines. Bars represent standard errors
(Based on Buth and Evans 1988)

cotton, peanuts and soybean which is similarly due to substantial increase in HI, emphasising (Gifford *et al.* 1984) that partitioning of photoassimilate rather than generation of whole-plant biomass was responsible for such yield improvement.

Carbon partitioning during reproductive development thus responds to sink strength which then impinges on final yield. Other important sources of variation in yield can be identified via a simple yield component model. Taking cereals as an example, final yield ((g grain) m^{-2}) will be a product of ears per square metre (ears m^{-2}), grains per ear and mass per grain. Ears m^{-2} is in turn an outcome of planting density (plants m^{-2}), tillers per plant and ears per tiller.

Some yield components such as mass per grain are especially stable, others such as ears m^{-2} and grains per ear vary widely with seasonal conditions or according to original planting density (Table 6.11). In that case (*Insignia* wheat at Glen Osmond, South Australia), mass per grain was highly conserved (33–35 mg) whereas tillers per plant varied from 41 at lowest planting density to only three at highest density. Significandy, yield variation was buffered by compensatory responses in yield components. For example, effects of low planting density were offset by production of more tillers per plant and more ears per tiller. Grains per ear then determine potential yield so that growing conditions would have become crucial for realising such potential via grain retention and filling.

Genotype × environment interactions lead to huge variation in cereal grain yield and have been exploited for yield improvement. Universally, high grain number per square metre is a prerequisite for high yield and can be achieved via more ears per square metre and/or more grains per ear. In wheat and barley, grain number per ear has been primarily

Table 6.11 Yield components of wheat (cv Insignia 49) sown in a red-brown earth at the Waite Institute, South Australia, varied according to planting density. Mass per grain is highly conserved, but plant mortality plus compensatory response between tiller number per plant, ears per tiller and grain number per ear buffers yield against variation in planting density

	Original density at planting (plants m^{-2})				
	1.4	7	35	184	1078
Density at harvest	1.4	7	35	154	447
Tillers per plant	41	30	14	7	3
Ears per tiller	0.7	0.6	0.5	0.3	0.2
Ears per sq. metre	41	130	252	323	303
Grains per ear	32.9	37.8	29.9	21.5	18.8
Mass per grain (mg)	34.2	35.0	32.7	33.2	33.1
Grain per plant (g)	33.2	24.7	7.05	1.52	0.42
Grain yield (g m^{-2})	46	173	247	234	185

Adapted from Puckridge and Donald (1967)

responsible for gains in yield; ears m^{-2} and mass per grain have not shown consistent increase (see Evans 1993 and literature cited).

Returning to collective outcomes represented by HI, one major impetus to improved shoot HI, in cereals came from the introduction of dwarfing genes. In primitive wheats, and tall plants generally, reproductive structures have to compete with rapidly extending stems for photoassimilate, but dwarf cultivars alleviate such competition and enable a shift in carbon partitioning to ears. Early growth of ears and stems in two lines of a Mexican spring wheat (Figure 6.25) illustrate this principle. A steeper slope in the dwarf line (designated *Rht 1+2*) com-

pared with the tall line (*rht*) implies greater allocation of photoassimilate to ear growth relative to stem growth. Expression of two dominant dwarfing genes in *Rht 1+2* (i.e. *Rht 1* plus *Rht 2*) resulted in stem shortening and was accompanied by an altered physiology where leaf and stem tissue proved insensitive to gibberellic acid. Such genotypes are reminiscent of dwarf wheats bred in Japan during the nineteenth century and used there for intensive cultivation (see Evans 1977).

Tall wheat commonly lodges in nitrogen-rich conditions, and dwarf wheats were originally developed to overcome this problem. Agronomists and crop physiologists subsequently recognised the yield advantage from improved partitioning of photoassimilate. Continuing selection for shoot HI in short bread wheats of northwest Mexico (Sayre *et al.* 1997) has resulted in grain yield increase from around 600 to almost 800 g m–2 between 1960 and 1990 (kernel number per square metre of land was also increased), while Watanabe *et al.* (1994) have documented comparative performance of Australian wheat cultivars developed between the 1850s and 1990s with similar conclusions. New cultivars outyielded old cultivars due to greater shoot HI rather than total biomass, while Austin *et al.* (1980) document genetic improvement of winter wheat in Britain over the preceding 80 years with a similar conclusion.

Modern hexaploid wheats are widely recognised as outyielding their diploid relatives due to higher HI and extended leaf area duration, but reduced photosynthetic capacity (area basis) has also been reported. Given such correlation, some researchers imagined there might even be a trade off between HI and leaf assimilation but lacked definitive information, and especially data on nitrogen-use efficiency. Leaf nitrogen is a key driving variable for photosynthetic activity and comparisons between genotypes or contrasts between successive developmental stages on a given plant need to accommodate variation in leaf nitrogen.

Evans (1985) clarified this issue by growing modern hexaploid wheat (*Triticum aestivum*) and less-developed diploid relatives (including *T. monococcum*) on high, medium and low nitrogen supply and then comparing light-saturated rates of photosynthesis as a function of leaf nitrogen on an area basis (Figure 5 in Evans 1985). Genetic differences were apparent, but in the critical comparison between *T. aestivum* and *T. monococcum*, gas exchange data overlapped almost completely, indicating no intrinsic difference in photosynthetic properties between these two species.

As expected in Evans's (1985) experiments, extensive tillering on high nitrogen in *T. monococcum* (52 heads per plant) resulted in higher grain yield (27.0 g per plant) compared with *T. aestivum* (12.3 g per plant). Nevertheless field trials showing greater HI in *T. aestivum* were confirmed by these pot experiments where *T. aestivum* returned 0.50 cf. 0.31 in *T. monococcum*. Superior field yield in hexaploid wheats can thus be attributed to a greater shoot HI and leaf area duration with no trade off in photosynthetic capacity.

Shoot HI has become an important selection criterion for plant breeders and focuses our attention on where shoot HI will eventually plateau. Enlarged ears or panicles call for robust stems, while generating photoassimilate necessitates a canopy, so that investment in vegetative organs will remain substantial and will impose a ceiling on shoot HI which is estimated at about 0.62 for wheat (Austin *et al.* 1980).

Clearly some room still exists for further improvement in shoot HI compared with 1980's values (Figure 6.24) but there is a corollary. If shoot biomass continues to remain unchanged, further improvement in HI implies some reduction in leaf + stem mass. Considering leaves, SLA will have a finite limit for structural reasons so that the area of CO_2-assimilating tissue servicing those enlarged sinks must also reduce as mass is reduced. Net assimilation per unit area (NAR) will therefore need to increase even further if potentially higher yields are to be realised.

To this end, NAR can be regarded as a product of inherent capacity for net photosynthesis which is expressed to a greater or lesser extent according to canopy light climate. Significantly, net photosynthesis embodies respiratory losses where both gain and loss of photoassimilate are a further expression of genotype × environment interactions and are subject to human selection pressures. Variation in community NAR, and thus prospects for further improvement in net carbon assimilation, can come from either photosynthetic or respiratory sources. Crop growth analysis (Section 6.4) deals with canopy architecture and light climate as factors in carbon gain, while growth efficiency and respiration (Section 6.5) covers carbon losses.

6.4 Crop growth analysis

Growth indices devised with single (isolated) plants (Section 6.1 *et seq.*) have helped identify genetic and environmental factors as sources of variation in NAR and/or LAR with consequences for RGR of both whole plants and their component organs. Leafiness was seen as a self-evident and important force for single plants when grown free from interference by neighbouring plants, and was quantified as LAR. However, plants rarely complete their life cycles as isolated individuals in either natural or managed ecosystems, growing instead as communities where mutual interference cannot be avoided. Biomass formed per unit area of land is then of more practical relevance than productivity per plant.

6.4.1 Concepts

By analogy with single plants growing exponentially where RGR = NAR × LAR (Equation 6.12), instantaneous rate of dry matter production by a community of plants or crop growth rate (CGR, sensu Watson 1958) can be summarised as

$$CGR = NAR \times LAI \quad (6.19)$$

where LAI or leaf area index (sensu Watson 1947) is a dimensionless ratio of total (projected) leaf area per unit ground area.

Some crops do sustain gas exchange on both leaf surfaces (amphistomatous) but LAI relates more fundamentally to light absorption than to CO_2 assimilation and is always based on total projected leaf area (i.e. single-sided leaf area).

RGR of single plants (d^{-1}, or more explicitly g g^{-1} d^{-1}) and absolute growth rate of a plant community, or CGR (g m^{-2} d^{-1}), are interrelated. For a given crop biomass (g m^{-2}) the collective RGRs of individuals in a crop translate to CGR where

$$CGR = Biomass \times RGR \quad (6.20)$$

Put more explicidy with A as canopy area, W as plant mass, N as the number of plants per unit ground area and dW/dt as rate of total biomass accumulation per unit time (t), then:

$$N\frac{dW}{dt} = NW \times \frac{A}{W} \times \frac{1}{A}\frac{dW}{dt} \quad (6.21)$$

so that

$$CGR = Biomass \times LAR \times NAR \quad (6.22)$$
$$= Biomass \times RGR$$

6.4.2 Light-use efficiency

Again by analogy with growth analysis of single plants where LAR denotes 'leafiness' of individuals, LAI represents community leafiness and helps define light profiles within crop communities (cf. Section 1.1). Monsi and Saeki (1953) are credited with formalising an expression analogous to Beer's law and based on LAI for attenuation of light with depth in crop canopies, namely

$$I = I_0\, e^{-kL} \quad (6.23)$$

where I_0 is irradiance above a canopy and I is irradiance beneath a canopy of LAI = L. The extinction coefficient k ranges between about 0.2 and 1.8 according to size, pose and light absorption by individual leaves (larger values for big thick horizontal leaves and smaller values for small thin pendant leaves).

Notwithstanding wide variation in canopy architecture, Equation 6.23 provides a robust model for canopy light climate and accordingly CGR can now be expressed in functional terms where

$$CGR = I_0\,(1 - e^{-kL})\varepsilon \quad (6.24)$$

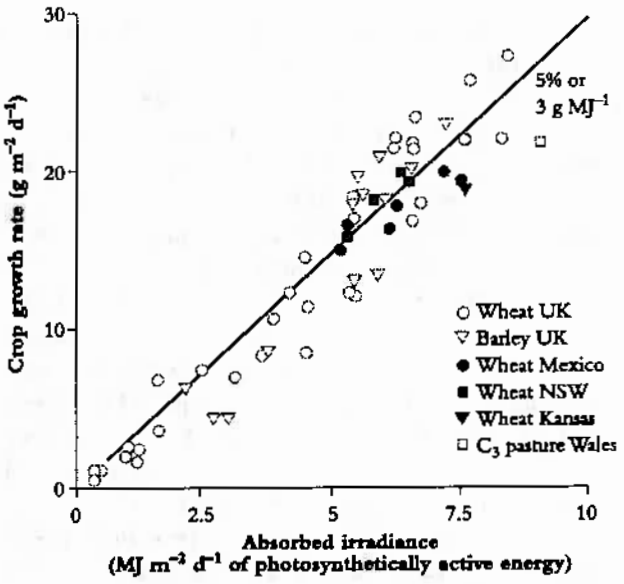

Figure 6.26 Crop growth rate (g dry matter m^{-2} d^{-1}) is linearly related to irradiance absorbed (MJ m^{-2} d^{-1}) for a wide range of crop communities. Efficiency of light utilisation (ε, g MJ^{-1}) is represented by the slope of that relationship and is equivalent to 3 g MJ^{-1} (or 5%) in this example
(Based on Evans 1993)

The terms in brackets (Equation 6.24) summarise light absorption whereas ε represents the efficiency with which absorbed light is utilised for dry matter production. ε is inferred from the slope of a relationship showing CGR as a function of absorbed light such as that in Figure 6.26. In that particular case, irradiance was used with about 5% efficiency in generating 3 g dry matter per MJ absorbed (i.e. ε = 3 g MJ^{-1}).

LAI (L in Equation 6.24) and extinction coefficient (k in Equation 6.24) will both vary according to leaf attributes, planting density and subsequent canopy development. Similarly, ε will vary according to mode of photosynthesis, nutrient supply and state of development. Typical values (Table 6.12) range from 4.15 in rice (C_3) or 3.40 in maize (C_4) down to 1.63 in clover and 1.29 (g MJ^{-1}) in soybean. High efficiency in rice and maize relate to inherently fast photosynthesis in well-nourished crops whereas an apparently low efficiency in clover and soybean reflect the carbon cost of biological nitrogen fixation and generally slower photosynthesis (area basis) in those species.

Table 6.12 Communities of crop plants vary widely in their efficiency of light utilisation for dry matter production (ε) due to differences in canopy architecture, photosynthetic attributes and respiratory losses

Crop species	ε (g MJ^{-1})
Rice (*Oryza sativa*)	4.15
Maize (*Zea mays*)	3.40
Sweet potato (*Ipomea batatas*)	3.06
Kale (*Brassica oleracea*)	2.65
Sunflower (*Helianthus annuus*)	2.59
Cotton (*Gossypium hirsutum*)	2.52
Sub clover (*Trifolium subterraneum*)	1.63
Soybean (*Glycine max*)	1.29

(Adapted from Warren Wilson 1969)

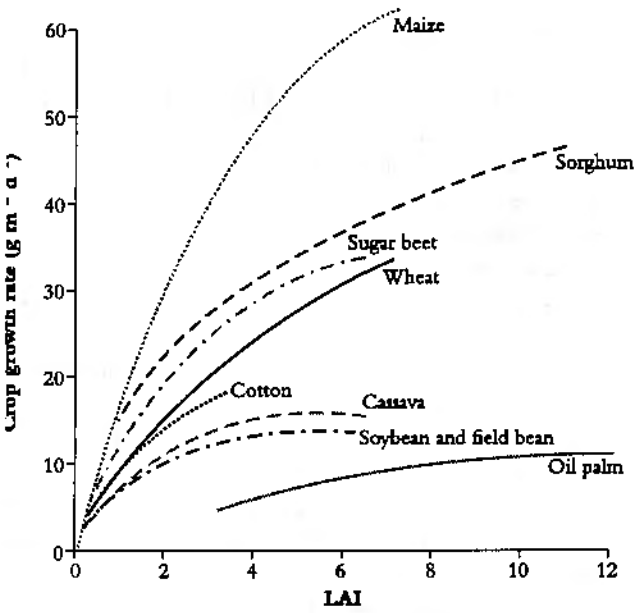

Figure 6.27 Crop growth rate (g dry matter m^{-2} d^{-1}) is a function of LAI (ratio of canopy area to ground area) where slope and asymptote vary according to light-conversion efficiency and canopy architecture
(Based on Evans 1993)

Crop growth data compiled from a number of sources (Figure 6.27) reveal LAI as a key driving variable, and especially prior to canopy closure where better illumination of individual plants is compounded by vigorous early growth and development. Radiation climate, canopy architecture and light-use efficiency would all contribute to these species differences, but in broad terms, low values for CGR in cassava and oil palm reflect annual averages and would increase somewhat if leaf litter had been included in above-ground biomass. Even so, perennial plants such as oil palm commonly photosynthesise more slowly than annual crop plants (leaf area basis) and thus achieve rather lower CGR. By contrast, C_4 photosynthesis in maize and sorghum obviously confers an advantage on these two species where an inherently high capacity for CO_2 assimilation is coupled with higher rates of leaf emergence and expansion plus more effective export of photoassimilate from source leaves. Net efficiency of light-energy conversion to biomass in this particular high-performance maize crop was around 8%, and somewhat higher than data cited in Table 6.12 with $\varepsilon = 3.40$ g MJ^{-1}, representing a light-energy conversion efficiency of 5.7%.

6.4.3 Potential crop growth rate

Genetic factors dictate potential yield, which in turn is set for every genotype by the intrinsic efficiency of light-energy conversion and net generation of photoassimilate. In wellnourished crops, yield is ultimately limited by community use of light energy. Such utilisation can be represented at successive levels of organisation (cf. Warren Wilson 1969) as follows. Take

Table 6.13 Dry matter production collated for a number of natural and managed ecosystems shows wide variation according to habitat conditions. Peak daily rates during growing seasons are commonly much higher with crops ranging between 5 and 15 g m^{-2} d^{-1}, and natural ecosystems between 1 and 10 g m^{-2} d^{-1}

Ecosystem	Annual productivity (g dry matter m^{-2} y^{-1})
Tropical	
Perennial crops	8000
Rainforest	3500
Annual crops	3000
Temperate	
Perennial crops	3000
Annual crops	2000
Grassland	2000
Evergreen forest	2000
Deciduous forest	1500
Savanna	1000
Arctic and arid	
Desert	100

(Adapted from Warren Wilson 1967, 1969)

an annual irradiance of 3.30×10^3 MJ m^{-2} y^{-1} as representative of mid-latitudes (10–30°). Consider a perennial tropical crop that maintains a complete canopy for 90% of each year, so that light energy available to that crop will be $0.9 \times 3.30 = 2.97 \times 103$ MJ m^{-2} y^{-1}. Taking LAI = 5 with an extinction coefficient k of 0.46 (recall Equation 6.24) intercepted energy will be $0.9 \times 2.97 = 2.67 \times 10^3$ MJ m^{-2} y^{-1}. Taking an efficiency of light-energy conversion to dry matter (ε) of 4.15 g MJ^{-1} (recall rice in Table 6.12), dry matter production should be $4.15 \times 2.67 \times 10^3$ or about 11 000 g m^{-2} y^{-1}.

Compare that estimate with observed values for both natural and managed ecosystems (Table 6.13) where total dry matter production per year ranges from 8000 g m^{-2} y^{-1} in perennial tropical crops down to 1500 g m^{-2} y^{-1} in temperate deciduous forests. Soil–plant–atmosphere water relations, nutrient supply, canopy light climate and duration of growing season will all contribute *inter alia* to variation in Table 6.13, but limitations imposed by light-energy conversion efficiency will be common to all. Photosynthetic energy transduction has an absolute requirement for 8–12 quanta per molecule of CO_2 fixed, but this photochemical restriction is compounded to a varying extent by CO_2 diffusion limitations. Some scope thus exists for improving dry matter production via leaf physiology, and in greenhouse crops via CO_2 enrichment. Greenhouse microclimate is conducive to year-round production, with annual productivity commonly two to three times higher in greenhouse than in field, and even further enhanced under elevated CO_2. For example, Warren Wilson *et al.* (1992) compared ambient with CO_2-enriched greenhouse crops, and showed that mean efficiency of light utilisation (net photosynthesis per unit intercepted light) for a number of crop species increased from 8.06 to 10.90 μg CO_2 J^{-1}. By contrast, well-managed field crops returned on average only 7.10 μg CO_2 J^{-1}. Duration of cropping season would amplify these greenhouse–field differences even further in terms of annual productivity.

6.4.4 Respiratory losses

Notwithstanding genetic differences in component processes of photosynthesis, net efficiency of light-energy conversion to biomass will impose a ceiling on CGR. Respiratory losses will feature in that overall net efficiency must be included in any process-based model of crop growth. Taking well-documented cases of canopy light climate and combining those profiles with light response curves for photosynthesis by single leaves, early modellers further assumed that respiratory loss would also be proportional to LAI and predicted an optimum LAI for different crop types.

Experience showed otherwise (Figure 6.27) with CGR increasing asymptotically with LAI for a wide range of crop species rather than showing an optimum. Why is there this discrepancy between theory and practice? In a classic case where model making was no substitute for experimentation but did suggest what experiment had to be done, flawed estimates of respiration proved responsible.

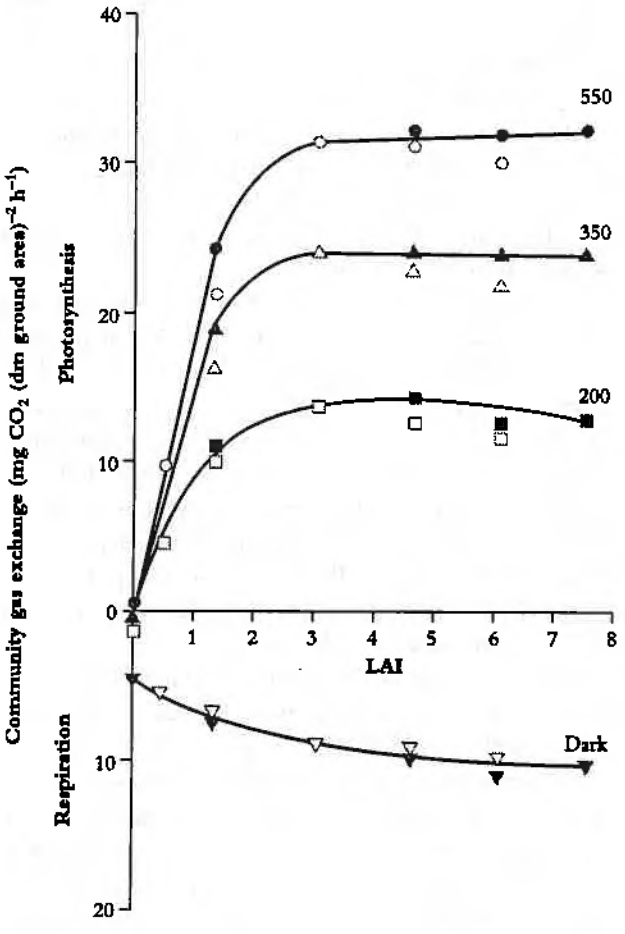

Figure 6.28 Community gas exchange by cotton plants in a growth cabinet (duplicate measurements at 20°C; low (200), medium (350)and high (550) photon irradiance (μmol m^{-2} s^{-1}) plus dark respiration as indicated) shows an asymptotic relationship to LAI (ratio of canopy area to ground area) with maximum net assimilation reached around LAI = 3.5. Additional measurements at higher temperatures (30°C and 40°C) amplified differences due to photon irradiance and showed some reduction in net photosynthesis at high LAI. Respiration at zero LAI represents CO_2 efflux from stems and roots (Based on Ludwig *et al.* 1965)

Using a highly novel approach to this issue, Ludwig *et al.* (1965) started with the intact canopy of an artificial community of cotton plants and varied LAI by removing successive layers of foliage from bottom to top. They demonstrated that respiratory losses from lower (shaded) leaves in artificial cotton communities downregulated in proportion to light attenuation. Lower leaves, both older and more shaded than their better-exposed counterparts towards the top of a canopy, thus impose a smaller respiratory load than would be predicted by LAI alone. Consequently, daytime CO_2 assimilation (net photosynthesis) and night-time respiratory loss by an entire community both show an asymptotic relationship with increased LAI (Figure 6.28). King and Evans (1967) subsequently confirmed this same relationship for artificial communities of wheat, lucerne and subterranean clover where community net photosynthesis approached a maximum at LAI values of about 8, 9 and 5 respectively.

By implication, there is no clear optimum LAI for CGR either, although harvest index (shoot HI in Section 6.3.3) can decrease in dense plantings (high LAI) due to restrictions on reproductive development by individual plants. Grain yield per unit area of land can thus show an optimum LAI even though CGR tends to an asymptote.

Respiratory costs associated with plant growth and reproductive development are thus crucial to both biomass accumulation and yield outcomes, representing a surprisingly large fraction of carbon fixed by leaf assimilation and especially under suboptimal growing conditions. Genetic differences in respiratory efficiency thus interact with environmental conditions in determining growth and reproductive success in nature as well as the comparative performance of crop plants. Underlying processes responsible for such differences in production and utilisation of respiratory energy are discussed in Section 6.5.

6.5 Respiratory efficiency and plant growth

Production of photoassimilate depends upon capture of light energy but subsequent use by plants necessitates expenditure of metabolic energy. Fixed carbon meets this need, so that costs associated with growth and maintenance of vascular plants can be represented as biomass equivalents. Generalised values for such dry matter utilisation during growth and development (Table 6.14) show that respiratory demand is substantial. According to these estimates, a germinating seedling with starting biomass of 1 g would in one day gain a further 0.2 g in structural growth plus 0.05 g in storage, resulting in an RGR of 0.25 g g^{-1} d^{-1}. However, respiratory losses supporting that strong RGR would have been equivalent to 0.10 g g^{-1} d^{-1}. Using similar logic, the young vegetative plant in Table 6.14 has achieved an RGR of 0.2 g g^{-1} d^{-1} at a respiratory cost equivalent to 0.08 g g^{-1} d^{-1}, and in a mature plant

with storage organs that are importing photoassimilate, RGR has fallen to 0.15 g g^{-1} d^{-1} with a respiratory cost equivalent to 0.04 g g^{-1} d^{-1}.

During such growth and development (Table 6.14) a downward drift in RGR has been accompanied by a similar fall in whole-plant respiration, although component costs have changed. Structural growth decreased whereas storage increased. Overall, respiration accounts for a significant fraction of photoassimilate. Commonly one-third and under stressful conditions as much as two-thirds of a plant's daily fixed CO_2 can be respired during the same period (Van der Werf *et al.* 1994).

Table 6.14 Generalised values for dry mass utilisation relative to whole-plant mass (g g^{-1} d^{-1}) at three stages of development from germination to maturation. New photoassimilate generated each day is allocated to growth, storage and respiration in biomass equivalents relative to each gram of existing biomass, as shown. Embryo growth in the germinating seedling is drawing on seed reserves that were not included in these notional calculations

Stage of development	Growth	Storage	Respiration
Seedling (germinating)	0.20	0.05	0.10
Vegetative growth	0.15	0.05	0.08
Maturation and storage	0.05	0.10	0.04

(Adapted from Warren Wilson 1969)

Processes supporting a net gain in new biomass (dW, g) per unit time (dt, d) can be represented as:

$$\frac{dW}{dt} = A - R \qquad (6.25)$$

where A is daily carbon assimilation and R is whole-plant respiratory loss, so that net gain per unit existing plant biomass per unit time (or RGR, g g^{-1} d^{-1}) becomes

$$RGR = \frac{1}{W}\frac{dW}{dt} = \frac{A}{W} - \frac{R}{W} \qquad (6.26)$$

If A and R are expressed as mmol carbon g^{-1} dry matter per day, then Equation 6.26 becomes

$$RGR = (A - R)/C_{wp} \qquad (6.27)$$

where C_{wp} is plant carbon concentration in mmol C (g dry matter)$^{-1}$.

A and R can be determined from direct measurement of whole-plant gas exchange, and the example below uses a value of 34.8 mmol C (g plant)$^{-1}$. Whole-plant RGR can now be linked to gas exchange data for shoot assimilation (A), shoot respiration (R_{shoot}) and root respiration (R_{root}) according to the expression

$$RGR = (A - (R_{shoot} + R_{root}))/C_{wp} \qquad (6.28)$$

6.5.1 Carbon economy of fast- versus slow-growing plants

An inherent capacity for fast growth confers a selective advantage on plants in favourable environments such as warm moist lowlands, but would be selectively neutral in restrictive environments such as nutritionally poor sites or alpine regions. Accordingly, fast-growing species achieve a higher RGR under optimum conditions than do slow-growing species under similar conditions. In either case, carbon loss via respiration is considerable with genetic differences in generation and utilisation of respiratory energy contributing to these differences in RGR.

Fast-growing species achieve a higher RGR than slow-growing species because their net rate of CO_2 uptake per unit of shoot and whole-plant mass is greater (Figure 6.29). By definition, net carbon fixed per day must depend to some extent on the proportion of fixed CO_2 that is subsequently lost by respiration, so that differences in respiratory CO_2 loss have an important impact on net carbon gain, and can be linked quantitatively to RGR. Data shown in Figure 6.29 can be used to calculate RGR for each species at the time of photosynthesis and respiration measurements if the plant's

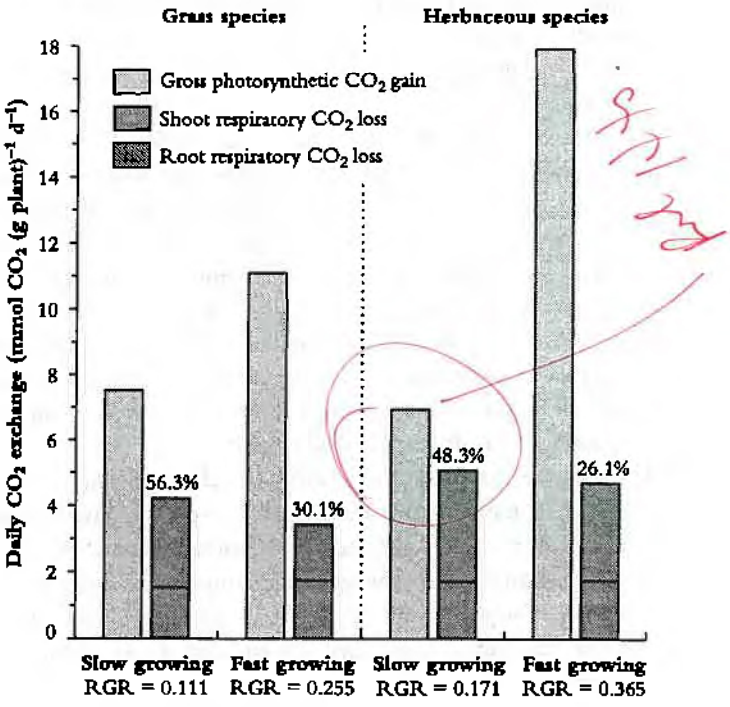

Figure 6.29 Daily carbon economy of plant species that differ with respect to inherent maximum RGR (g g^{-1} d^{-1}). The fast-growing grass and fast-growing herb both exhibit higher rates of gross photosynthetic CO_2 uptake per unit plant mass (i.e. net photosynthesis plus shoot dark respiration) than their slow-growing counterparts. Fast-growing species lose a smaller percentage of daily fixed carbon via respiration (values shown above each respiration bar)

(Based on data in Atkin *et al.* (1996) for slow-growing Australian alpine and fast-growing lowland *Poa* species, and Poorter *et al.* (1990) for the slow-growing herb *Pimpinella saxifraga* versus the fast-growing herb *Galinsoga parviflora*)

carbon concentration is known. As outlined above, RGR is related to photosynthesis, respiration and carbon content where

$$\text{RGR} = (\text{Daily } CO_2 \text{ gain} - \text{Daily } CO_2 \text{ loss by roots and shoots})/(\text{Carbon concentration}) \quad (6.29)$$

Taking the fast-growing grass in Figure 6.29, RGR = 0.22 g g^{-1} day^{-1} according to:

$$\text{RGR} = (11.1 - (1.75 + 1.68)\ \text{mmol C g}^{-1}\ \text{plant d}^{-1})/(34.8\ \text{mmol C g}^{-1}\ \text{plant}) = 0.22\ \text{g plant g}^{-1}\ \text{plant d}^{-1} \quad (6.30)$$

This prediction of 0.22 d^{-1} for RGR represents an instantaneous value derived from whole-plant gas exchange measurements, whereas 0.255 in Figure 6.29 represents an average RGR from growth analysis over several days. Gas exchange values are generally within 10% of RGR values from sequential harvests.

Net carbon gain per day and hence NAR is clearly a consequence of daily photosynthesis minus whole-plant respiratory loss, but herbs and grasses differ in the degree to which respiratory losses account for differences in RGR. Considering grasses (Figure 6.29 left side), 56% of daily fixed CO_2 is lost by respiration in the slow-growing alpine species whereas only 30% of daily fixed CO_2 is respired by the fast-growing lowland grass species. Over half of the carbon loss is attributable to roots in both species and, overall, respiration rate per unit plant mass is slightly higher in the slow-growing grass species.

Herbs in Figure 6.29 (right side) differ from grasses because the fast-growing herb respires faster than the slow-growing herb (on a mass basis) so that differences in percentage loss of carbon between these species cannot be due to differences in respiration rates *per se*. Significantly, however, the fast-growing herb still loses a smaller percentage of daily fixed carbon due to whole-plant respiration because daily CO_2 assimilation (mass basis) is especially high. A notably higher SLA in this fast-growing herb contributes to faster photosynthesis on a mass basis (Figure 6.29).

A lower percentage loss of daily fixed carbon due to respiration in fast-growing grasses and fast-growing herbs does imply that carbon metabolism is more effective in these species than in their slow-growing counterparts, and serves as a model for generalisations. Such fast-growing plants may be more efficient in how they *generate* and/or *use* respiratory energy.

6.5.2 Energy generation

Photoassimilate is used to generate respiratory products needed for plant growth (Figure 6.30). Carbon is exported from chloroplasts to the cytosol and mitochondria, and used to generate ATP, redox equivalents (in particular NADH) and carbon skeletons via glycolysis, mitochondrial tricarboxylic acid (TCA) activity and mitochondrial electron transport. Generation of these respiratory products necessitates CO_2 loss during glycolysis and passage of metabolites around the TCA cycle. Mitochondria subsequently facilitate electron transport from NADH or $FADH_2$ to ubiquinone (Figure 6.31). From there, electrons can be transferred via the cytochrome pathway to complexes III and IV, ultimately reducing O_2 to H_2O. Complex I, complex III and complex IV are all coupled to proton translocation and thus ATP synthesis. However, when electrons go via the NADH dehydrogenase step (rotenone resistant), or via succinate dehydrogenase (Complex II) or via the alternative oxidase pathway, protons are not translocated and thus ATP is not synthesised. Engagement of these non-phosphorylating pathways will result in loss of energy as heat without any accompanying yield of ATP. Heat generation by the Arum lily spadix (see Feature essay 2.2) is an extreme case of such thermogenesis.

Conceivably, plants which contrast in RGR also differ in the degree to which they engage alternative versus cytochrome pathways, but definitive evidence is still lacking. Existing estimates of electron partitioning between the alternative and

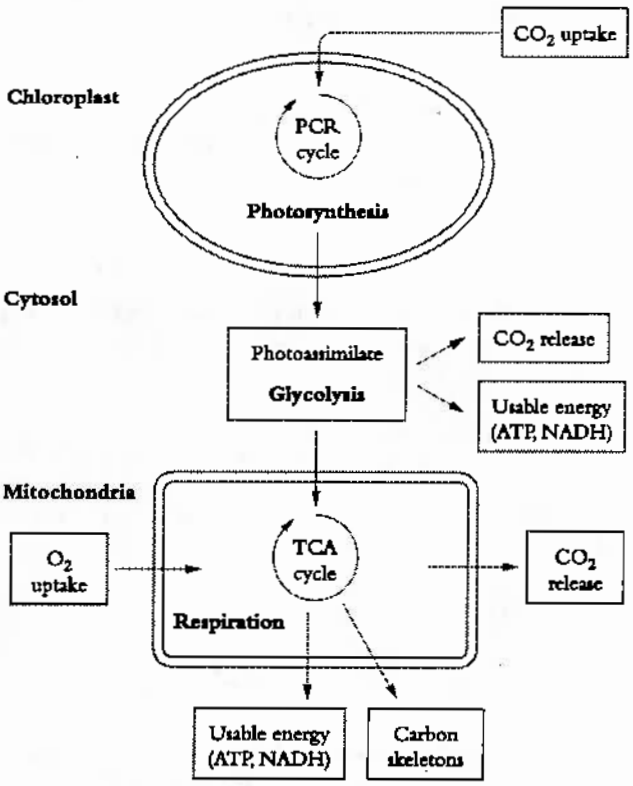

Figure 6.30 Simplified view of processes involved in carbon gain and generation of respiratory energy. CO_2 assimilated by chloroplasts is used to produce carbon-rich compounds (photoassimilates) that are subsequently exported to the cytosol and mitochondria. CO_2 is then lost during breakdown of these carbon-rich compounds by glycolysis and mitochondrial respiration. Release of CO_2 and uptake of O_2 by mitochondria are coupled to production of usable energy (ATP, NADH). Carbon skeletons (necessary for protein synthesis) are also produced during mitochondrial respiration
(Original drawing courtesy Owen Atkin)

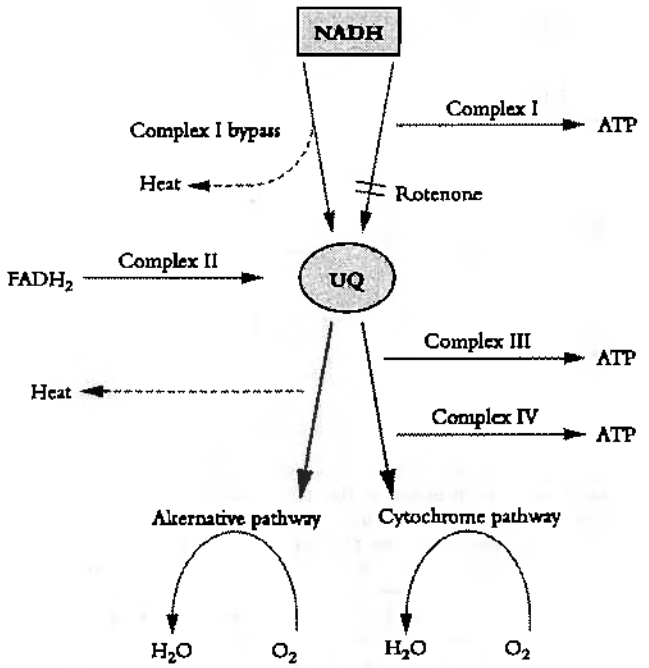

Figure 6.31 Pathways of electron transport on the inner membrane of plant mitochondria. Electrons from NADH or $FADH_2$ are transferred to the ubiquinone pool (UQ) via complexes I and II, respectively. Electrons can then be transferred to O_2 via either the alternative pathway or via complex IV in the cytochrome pathway. Energy is ultimately conserved as ATP whenever electrons pass via complex I, complex III or complex IV. In contrast, energy is lost as heat when the complex I bypass or alternative pathway is engaged. The alternative pathway can be inhibited by salicylhydroxamic acid (SHAM), whereas the cytochrome pathway is inhibited by cyanide
(Original drawing courtesy Owen Atkin)

cytochrome pathways based on respiratory inhibitors such as cyanide and solicylhydoxamic acid (SHAM) (Figure 6.31 legend) are ambiguous (see Millar *et al.* 1995a; Hoefnagel *et al.* 1995). Nevertheless, theoretical implications of alternative versus cytochrome pathway engagement can be calculated. Fast- versus slow-growing species would differ in the efficiency of ATP generation. An efficient, fast-growing species could generate 32–36 molecules of ATP for each molecule of glucose that enters glycolysis provided all the electrons pass through complex I to the ubiquinone pool and then 100% go via the cytochrome pathway. Less ATP is produced (i.e. 32 molecules) if glycolytic NADH is used for cytosolic reduction processes whereas more ATP is produced (i.e. 36 molecules) if glycolytic NADH goes to ATP production in mitochondria. By contrast, in an inefficient slow-growing species, diversion of 70% of electrons in the ubiquinone pool to the alternative oxidase (with only 30% passing via the cytochrome pathway) would result in only 16–18 molecules of ATP being generated per molecule of glucose.

Variations in engagement of the alternative oxidase (or other non-phosphorylating pathways) could thus have a significant impact on ATP generated per mole of CO_2 released during respiration. Slower respiration in fast-growing species (e.g. the herb in Figure 6.29) could be due in part to increased efficiency of energy generation due to greater engagement of the cytochrome pathway.

6.5.3 Energy utilisation

Fast-growing species could also use respiratory energy more efficiently for maintenance, growth and ion uptake. Variations in efficiency of energy use reflect differences in the proportion of whole-plant respiration that is allocated to these three processes and/or the specific costs of each process (Amthor 1989).

Maintenance respiration represents the portion of respiratory CO_2 release that is coupled to (1) production of energy (ATP and reducing power) necessary for maintenance of chemical and electrochemical gradients across membranes, (2) turnover of cellular constituents such as proteins and (3) processes involved in physiological acclimation to changing or harsh environments (Penning de Vries 1975). Energy needed for maintenance is controlled by the specific costs of processes taking place and is generally regarded as proportional to tissue mass.

Protein turnover is an energy-intensive process accounting for 60–80% of maintenance respiration (Penning de Vries 1975). Demand for respiratory energy associated with protein turnover will depend on turnover rate, respiratory costs associated with turnover, as well as the total amount of proteins undergoing turnover. Enzymes such as nitrate reductase (a key enzyme involved in nitrogen assimilation) have a very high turnover rate (Amthor 1984). As a result, plants assimilating nitrate have higher maintenance requirements than ammonium-grown plants (Hansen 1979).

Translocation of photoassimilate is also a potentially expensive process that accounts for approximately 30% of total dark respiration in several starch-storing plant species (Bouma 1995) and would represent a substantial drain on photoassimilate that could otherwise go into storage organs (Table 6.14). Phloem loading and uuloading is largely responsible for this high cost because transport of sugars between symplasm and apoplasm depends on cotransport of H^+. Movement of H^+ is in turn dependent on ATP being consumed in the symplasm (Chapter 5). Traffic in photoassimilate thus increases demand for maintenance respiration

Energy costs associated with nutrient aquisition are often very high because ions have to be transported across root cell membranes using active transport systems that require substantial amounts of ATP. Energy requirement for ion uptake will depend on several factors, including the degree to which absorbed nutrients are released back to the soil and the degree to which protons and anions are cotransported into roots.

Growth respiration covers synthesis of new biomass from photosynthate and mineral nutrients and is regarded as proportional to the rate at which new material is being formed. Specific respiratory costs associated with growth (i.e. construction cost) will depend to a large extent on the chemical composition of plant material and by implication the amount of energy embedded in these molecules (Table 6.15). Compounds with a high carbon concentration require more ATP and reducing power for their synthesis (Lambers and Poorter

Table 6.15 Construction costs (grams of glucose needed to synthesise a gram of a given compound) for different groups of compounds in plant tissues

Compound	Construction costs
Lipids	3.030
Lignin	2.119
Protein (using NO_3^-)	2.475
Protein (using NH_4^+)	1.623
Cellulose	1.220
Non-structual carbohydrates (e.g. sucrose)	1.090
Organic acids	0.906
Mineral uptake	0.100

(Adapted from Poorter 1994; Penning de Vries *et al.* 1974)

1992). For example, biomass stored as lipid represents an investment of almost three times as much energy as would be required for storage of the same mass of non-structural carbohydrate. Plant growth analysis based on dry mass accumulation takes no account of such differences in chemical composition of end-products, so that comparisons of growth efficiencies based solely on RGR of biomass must be viewed circumspectly.

Construction cost, and thus growth respiration, also varies according to the chemical form of available nitrogen (e.g. N_2, NO_3^- and/or NH_4^+) *and* sites of assimilation. Nitrogen reduction is an energetically expensive process, requiring considerable input of respiratory energy (e.g. ATP + reductant) and TCA cycle intermediates. Plants fixing atmospheric N_2 in their roots demand much ATP, namely 12.5–26.5 mol ATP per mol of NH_4^+ produced, and a further 2.5–3.0 mol ATP for subsequent assimilation into nitrogen-based metabolites such as amino acids and proteins. NO_3^- reduction to NH_4^+ is cheaper, costing around 12 mol ATP per mol NH_4^+ produced.

Respiratory costs associated with NO_3^- assimilation can be substantially reduced if reduction of NO_3^- to NH_4^+ and subsequent assimilation of NH_4^+ into amino acids takes place in leaves. Reduction and assimilation of NO_3^- can then utilise excess photosynthetic reductant and ATP. Growth respiration associated with synthesis of nitrogen-based resources is thus greatly reduced by shoot assimilation of NO_3^-. Sun-adapted (fast-growing) plants show this feature (Chapter 16).

6.5.4 Methodology

Growth respiration can be distinguished from maintenance respiration by relating variation in respiration rate to variation in RGR over short time intervals (Figure 6.32; Penning de Vries 1975). This approach assumes a model for respiration where:

$$\text{Respiration rate} = \text{Maintenance respiration} + \text{Specific costs of growth} \times \text{RGR} \quad (6.31)$$

Decreases in RGR (e.g. due to growth under different irradiance or during ageing) are assumed to decrease demand for

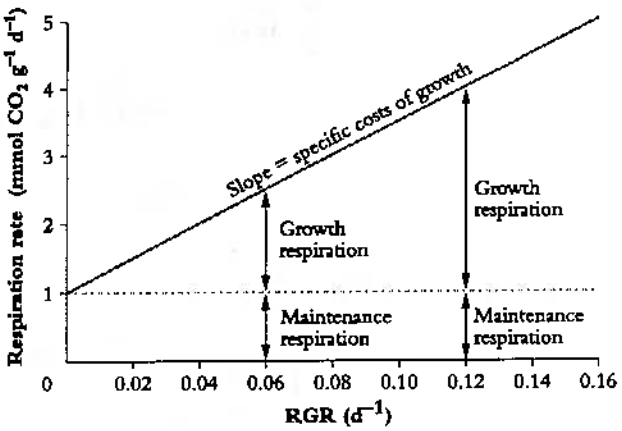

Figure 6.32 Determination of growth and maintenance respiration in whole plants, roots or shoots. Respiration rates are plotted as a function of RGR and maintenance respiration is taken as the rate of respiration when RGR is extrapolated to zero. The slope of this plot (25 mmol CO_2 g^{-1}) provides an estimate of the specific costs of growth which are assumed to remain constant for a given plant regardless of RGR. Variation in both RGR and respiration rate can be generated in several ways, including growing plants under different irradiances, or by measuring respiration and growth rates during development (RGR and respiration rate commonly decrease with age)
(Original drawing courtesy Owen Atkin)

growth respiration, whereas demand for maintenance respiration is assumed to remain constant at different RGR values. Based on these assumptions, the maintenance component can be estimated by extrapolating the respiration rate back to a point where no growth occurs (1 mmol CO_2 g^{-1} d^{-1} in Figure 6.32). Specific respiratory costs associated with growth can be estimated from the slope of the respiration–RGR plot (25 mmol CO_2 g^{-1} in Figure 6.5.4).

An alternative approach to maintenance and growth components of respiration involves holding plants in extended darkness. Most annual plants use up their readily available energy sources after about 2 d and shoot growth will cease. Rate of CO_2 release would then reflect the maintenance component of dark respiration. The difference in dark respiration rates before and after 2 d darkness would be the growth component.

Such methods incorporate specific costs of ion uptake into estimates of growth respiration, but do not isolate the ion uptake component of root respiration. Ion uptake respiration can be separated from growth by partitioning root respiration into growth, maintenance and ion uptake components. The approach adopted by Veen (1980) assumes a model where

$$\text{Root respiration rate} = \text{Maintenance respiration} + \text{Specific costs of growth} \times \text{Root relative growth rate} + \text{Specific costs of ion uptake} \times \text{Ion uptake rate} \quad (6.32)$$

A multiple regression analysis approach can be used to separate these components (Figure 6.33). Root respiration is taken as a dependent variable; while RGR and ion uptake rate are independent variables (Van der Werf *et al.* 1994). The maintenance component of root respiration is taken as the rate of respiration when growth and ion uptake are extrapolated back

to zero. Specific costs of growth and ion uptake are taken as the slope of the respiration versus growth and ion uptake regressions, respectively.

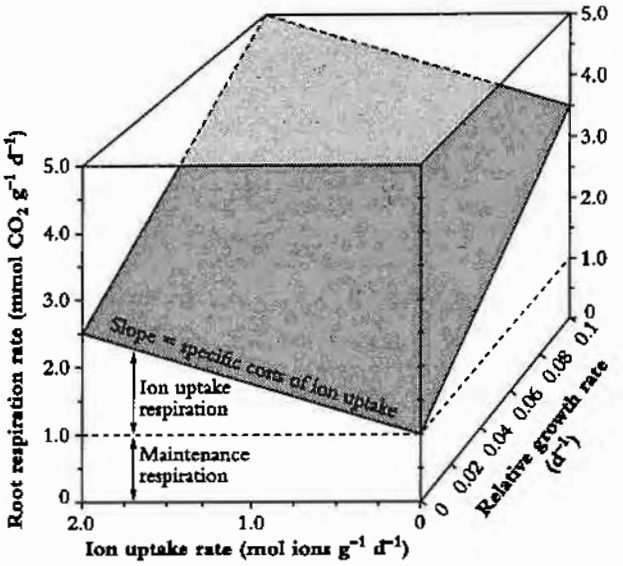

Figure 6.33 Determination of growth, maintenance and ion uptake components of root respiration. Maintenance respiration is taken as the rate of respiration when ion uptake rate and relative growth rate (RGR) are extrapolated to zero. Specific costs of ion uptake are estimated from the slope of the respiration versus ion uptake rate plot, while the actual amount of respiration allocated to ion uptake is shown. The slope of respiration versus RGR represents the specific costs of growth. Growth respiration varies with RGR, but specific costs of growth, ion uptake and maintenance are assumed to remain constant irrespective of variation in RGR or ion uptake
(Original drawing courtesy Owen Atkin)

6.5.5 Energy use by roots

Most respiratory energy is allocated to nutrient acquisition in both fast- and slow-growing species (Figure 6.34) and this proportion increases even further under suboptimal conditions as maintenance costs rise. However, one key difference remains. Fast-growing species allocate less respiratory energy to nutrient aquisition, and more to growth. Presumably, a lower allocation to ion uptake in the fast-growing species implies lower specific costs. Loss of absorbed nutrients could also be lower in fast-growing species, while the degree to which protons and anions are cotransported into roots could be greater. Maintenance costs also appear to be slightly lower in fast-growing plants (Figure 6.34) but any difference between these two plant categories in allocation to maintenance processes is small and is unlikely to matter overall. Nevertheless, differences in maintenance respiration will become more important when a plant is exposed to unfavourable conditions which invariably increase allocation of respiratory energy to fine-root turnover and maintenance of those structures.

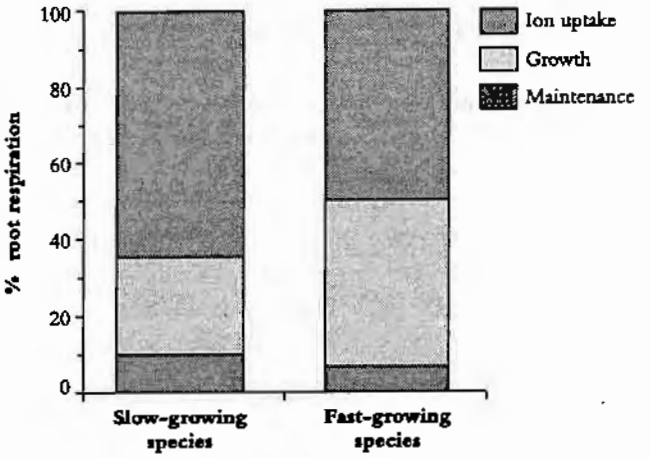

Figure 6.34 Root respiration is largely devoted to ion uptake and maintenance in slow-growing species (left side) compared with a predominant allocation to growth in fast-growing species (right side). (Generalised values comparable to Figure 6.29)
(Based on Poorter *et al.* 1991)

6.5.6 Growth efficiency and crop selection

A priori, increased respiratory efficiency via either energy production or utilisation should impact on RGR, and some selection has been attempted. Wilson and Cooper (1969) first demonstrated that wide variation in RGR among *Lolium perenne* (perennial ryegrass) populations from diverse habitats was attributable to differences in NAR. Wilson (1982) subsequently suggested that improved growth (10–20% increase in yield) of *L. perenne* grown in high-density swards could be achieved by genotypes whose mature leaves respired more slowly. Mature leaves had been selected as a measurement criterion in the belief that maintenance respiration would predominate compared with growth respiration.

Wilson (1982) and Robson (1982a,b) found genetic variation in maintenance respiration where slower dark respiration accounted for greater dry matter production, prompting the expectation that low maintenance requirements would generally increase the amount of fixed CO_2 that could be invested in growth. High-density swards of ryegrass behaved this way, but sadly the relationship between low respiration rates and improved growth disappeared when perennial ryegrass was grown as low-density swards (Kraus *et al.* 1993). Similarly, fast-growing pea cultivars exhibit less alternative pathway respiration than slow-growing cultivars in some studies (Musgrave *et al.* 1986) but not in others (Obenland *et al.* 1988). In view of such experiences, selection for faster RGR via respiratory efficiency due either to reduced alternative oxidase activity and/or decreased costs remains an attractive goal, but useful outcomes are not yet assured. Selection criteria will certainly have to be based on respiratory features that are maintained under a variety of growth conditions.

6.5.7 Suboptimal environments

Nitrogen limitation decreases absolute rates of shoot and root respiration in both fast- and slow-growing species (Figure 6.35) but the percentage of daily fixed CO_2 lost during respiration increases. Such increase on low nitrogen results from a greater allocation of photoassimilate to roots which in turn show an intrinsically higher rate of respiration (mass basis). Slower growth of whole plants on low nitrogen is therefore due to slower photosynthesis (mass basis) coupled with more costly nitrogen acquisition.

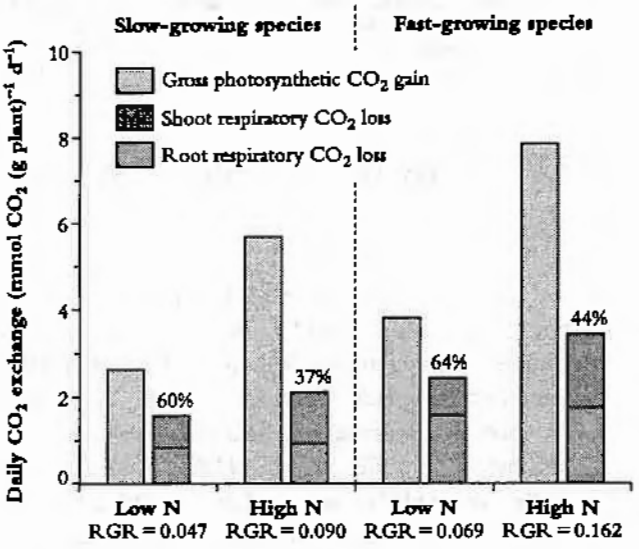

Figure 6.35 Low nitrogen (supplied as nitrate) reduces RGR in both fast-growing and slow-growing grass species. Photosynthesis and respiration (mass basis) also decrease, but the percentage of daily fixed carbon that is lost via respiration is increased, especially in the slow-growing grass. The percentage of daily fixed carbon lost via respiration (values above respiration bars) is higher on low nitrogen due to a greater investment of photoassimilate in roots. Photosynthetic CO_2 gain is expressed as net photosynthesis plus shoot respiration (assuming shoots respire in daytime at the same rate as that measured in darkness). Values for CO_2 exchange per unit plant mass were calculated from whole-plant measurements and proportions of plant biomass allocated to shoots and root, respectively
(Based on Poorter *et al.* 1995)

The proportion of daily fixed carbon that is respired will also increase under other stressful conditions such as excess salt or aluminium. Challenged by such stresses, plants increase their demand for energy to exclude the toxic compound or repair damage, and grow more slowly. For example, wheat roots increase respiration rates and grow more slowly due to high concentrations of aluminium (Collier *et al.* 1993). According to this model, a greater proportion of respiratory energy is being used to support cellular maintenance in place of growth under stressful conditions.

6.6 Concluding remarks

Ironic as it might seem, growth indices discussed here are not fundamental entities with some intrinsic significance for plants. Instead, they are derived concepts, and products of human intuition. As such they provide terms of reference for quantitative analysis of responses in growth and reproductive development at a single plant or community level, and sometimes point to processes responsible for those responses.

In most cases definition of a growth index is intuitive and inspired by features of growth occurring under conditions which allow exponential growth. A colonising population of single-celled organisms or simple floating plants such as *Lemna minor* can grow exponentially and thus in accordance with the law of compound interest. However, this is not the case with more complex vascular plants. In these, structural differentiation and a division of labour between tissues concerned with resource capture, substrate processing, structural integrity and photoassimilate storage leads to more complex growth patterns. Invariably, whole-plant RGR falls with age (size) even in a constant environment so that, in truth, whole-plant growth is probably never truly exponential, but fortunately these growth indices can still find application.

At any one time, growth indices and relationships between them yield information on plant function. More particularly, the manner in which these indices vary over time or in response to treatments points to changes in plant function during growth and development.

Decades of success in plant growth analysis has hinged upon shrewd insights and skilful construction and application of growth indices. Further refinement will emerge as improved measurements over shorter time intervals target component processes. Elaboration of conceptual or mathematical process-based models for plant growth and reproductive development will focus that effort, and eventually mechanisms responsible for genotype × environment interaction on gene expression in phenotypes will be identified and examined in more detail.

Further reading

Dale, J.E. (1982). *The Growth of Leaves: Studies in Biology 137*, Edward Arnold: London.

Evans, G.C. (1972). *The Quantitative Analysis of Plant Growth*, Blackwell Scientific Publications: Oxford.

Evans, L.T. (1993). *Crop Evolution, Adaptation and Yield*, Cambridge University Press: Cambridge.

Hunt, R. (1982). *Plant Growth Curves: The Functional Approach to Plant Growth Analysis*, Edward Arnold: London.

Lambers, H., Cambridge, M.L., Konings, H. and Pons, T.L. (eds) (1990). *Causes and Consequences of Variation in Growth Rate and Productivity of Higher Plants*, SPB Academic Publishing bv: The Hague.

Loomis, R.S. and Connor, D.J. (1992). *Crop Ecology: Productivity and Management in Agricultural Systems*, Cambridge University Press: Cambridge.

Part II

Processes and resources for growth

Part II Contents

7 *Plant growth and options for reproduction*

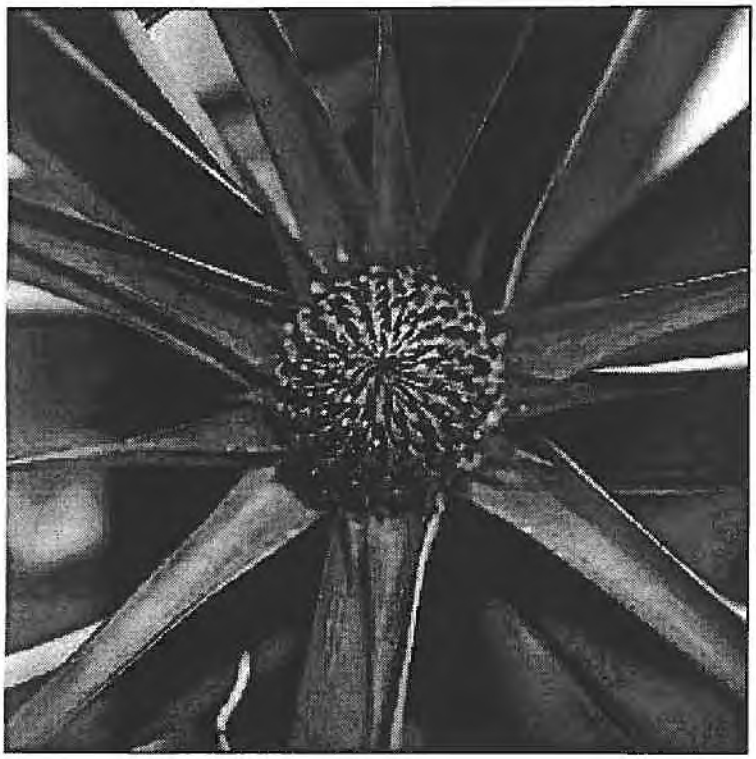

We should always keep in mind the obvious fact that the production of seed is the chief end of the act of fertilisation; anthat this end can be gained by hermaphrodite plants with incomparably greater certainty by self-fertilisation, than by the union of the sexual elements belonging to two distinct flowers or plants. Yet it is unmistakably plain that innumerable flowers are adapted for cross-fertilisation.

(Charles Darwin, The Effects of Cross and Self Fertilisation in the Vegetable Kingdom, 1876)

Figure 7.0 Developing pineapple inflorescence showing spiral phyllotaxis
(Photograph courtesy C.G.N. Turnbull)

Chapter outline